


**Elastic response of colloidal smectic liquid crystals: Insights from microscopic theory**H. H. Wensink <sup>1,\*</sup> and E. Grelet <sup>2</sup><sup>1</sup>*Laboratoire de Physique des Solides–UMR 8502, CNRS, Université Paris-Saclay, 91405 Orsay, France*<sup>2</sup>*Centre de Recherche Paul Pascal–UMR 5031, CNRS, Université de Bordeaux, 33600 Pessac, France*

(Received 31 January 2023; accepted 5 May 2023; published 24 May 2023)

Elongated colloidal rods at sufficient packing conditions are known to form stable lamellar or smectic phases. Using a simplified volume-exclusion model, we propose a generic equation of state for hard-rod smectics that is robust against simulation results and is independent of the rod aspect ratio. We then extend our theory by exploring the elastic properties of a hard-rod smectic, including the layer compressibility ( $B$ ) and bending modulus ( $K_1$ ). By introducing weak backbone flexibility we are able to compare our predictions with experimental results on smectics of filamentous virus rods ( $fd$ ) and find quantitative agreement between the smectic layer spacing, the out-of-plane fluctuation strength, as well as the smectic penetration length  $\lambda = \sqrt{K_1/B}$ . We demonstrate that the layer bending modulus is dominated by director splay and depends sensitively on lamellar out-of-plane fluctuations that we account for on the single-rod level. We find that the ratio between the smectic penetration length and the lamellar spacing is about two orders of magnitude smaller than typical values reported for thermotropic smectics. We attribute this to the fact that colloidal smectics are considerably softer in terms of layer compression than their thermotropic counterparts while the cost of layer bending is of comparable magnitude.

DOI: [10.1103/PhysRevE.107.054604](https://doi.org/10.1103/PhysRevE.107.054604)**I. INTRODUCTION**

Nonspherical colloidal particles or elongated molecules form liquid crystal mesophases with properties interpolating between those of a fluid, such as liquidlike diffusivity, and those of a crystal such as long-ranged periodic order [1]. Because of these hybrid properties, liquid crystals find widespread use in technological applications and knowledge of their phase behavior and mechanical response is of key importance in controlling and optimizing material properties composed of strongly nonspherical moieties [2]. Concepts of liquid crystal physics are also instructive to understand processes in the living cell [3,4] and to identify structures in biological matter [5].

Nematic phases are the simplest of such structures and are characterized by long-ranged orientational order of the particles, while lacking positional order in any direction. Moving one level up in order we find smectic-A– (SmA) type order that combines long-ranged stacking order along the main direction of particle alignment while retaining fluidity in the plane transverse to the layer normal. As such these lamellar structures can be interpreted in terms of a combination of unidirectional order and bidimensional fluidity which endows these materials with specific material properties owing to their distinct membranelike character [6–8].

As for the colloidal domain, phase transition among nematic, smectic, and other phases that may appear on variation of particle density have been the subject of intense theoretical study (the reader is referred to a number of excellent review papers on this topic [9–12]). Minimal models that

account for the stability nematic phases [13] and those with lower symmetry such as smectic [14] and columnar organizations [15,16] are based on simple uniaxial shapes (such as cylinders) that experience hard or steeply repulsive interactions.

For smectic materials, theoretical efforts have been aimed mostly at analyzing mechanical instabilities based on continuum theory where the underlying microscopic features of the particles are ignored. On the other hand, for rod-shaped colloids microscopic theories based on density functional concepts and simulations have primarily addressed the role of smectic order in the overall phase diagram of nonspherical colloids [14,17–19], subtle intralayer order [20], and, more recently, also their diffusive properties [21–23].

In this work, we aim to take a more in-depth look at colloid-based smectic liquid crystals taking hard-core cylinders as a benchmark model. We wish to address not only thermodynamic properties such as the equation of state but also various mesoscopic properties including the layer spacing, thermal corrugation of the smectic layers, and the elastic properties related to layer compression and layer bending. The latter are routinely described by the layer compression and bending moduli,  $B$  and  $K_1$ , respectively [1]. Our findings are relevant for a variety of colloidal smectic systems whose lamellar structure is stabilized primarily (but not exclusively) by hard-core volume exclusion such as TMV [24,25], TiO<sub>2</sub> [26],  $\beta$ -FeOOH [27], goethite [28], CdSe [29], and gold nanorods [30]. All smectic structures observed thus far were of the SmA or SmB type. While a SmA phase retains full intralayer fluidity, the SmB phase is characterized by long-ranged positional order of some kind within each layer. Examples of SmC type layering, in which the colloidal rods are tilted with respect to the layer normal, are scarce. Observations of ordering of this

\*rik.wensink@universite-paris-saclay.fr

kind have been reported for silica rods subjected to gravitational compression [31].

A number of recent experimental studies have been devoted to classifying topological defects in strongly confined colloidal smectics [32–34]. The symmetry and spatial extent of these defects depend strongly on the elastic properties of the smectic material which we intend to address here from a microscopic theoretical viewpoint. Further inspiration for undertaking a study of smectic elastic moduli stems from the emergence of advanced continuum theories for smectics [35–37] that rely on the elastic moduli to predict the response of layered materials to geometric frustration and other external stimuli.

Our approach is based on a two-way extension of the commonly employed cell theory for positionally ordered liquid crystals [38–42]. The first is a simple scaling description for a single lamellar fluid composed of near-parallel rods by decoupling the effects of orientational fluctuations from the parallel-core contribution. We demonstrate that the scaling approach gives a correct rendering of the onset of smectic and columnar order from a nematic melt for rod- and disk-shaped colloids alike. The second modification of the original cell-approach involves taking into account the out-of-plane fluctuations at the single-rod level and highlight their subtle role in determining the elastic properties of a smectic material, mostly in the layer bending modulus  $K_1$ . By suitably renormalizing quantities in terms of the individual rod dimensions we show that the equation of state and the elastic moduli of a hard-rod smectic can be rendered *independent* of the rod aspect ratio. In particular, we demonstrate that the smectic penetration length  $\lambda = \sqrt{K_1/B}$ , which should be interpreted as the intrinsic length scale over which elastic distortions such as edge and screw-dislocations relax in a lamellar system, does not primarily depend on the rod shape but only on the overall packing fraction of the smectic material.

We subsequently discuss the role of backbone flexibility of the rods which is relevant for filamentous virus rods and compare our predictions with experimental measurements on smectic phases of *fd* suspensions [21,43]. We find good agreement for the smectic layer spacing as a function of rod concentration as well as for the typical smectic potential that controls the single-rod diffusivity [44–46]. Last, we predict that the smectic penetration  $\lambda = \sqrt{K_1/B} \approx 0.02L$  is only a fraction of the rod length  $L$  and the smectic layer distance, in excellent agreement with measured values for *fd*. This illustrates that a hard-rod smectic has a different mechanical response than the more commonly explored molecular-based lamellar systems, such as lipid membranes [47] and thermotropic smectics where the smectic penetration length was found to be comparable to the lamellar periodicity [1,48–50]. We demonstrate that this discrepancy is chiefly due to colloidal smectics having a considerably smaller layer compressibility modulus than their thermotropic counterparts.

The remainder of this paper is organized as follows. In Secs. II and III we discuss a density-functional theory for a lamellar fluid by allowing for Gaussian out-of-plane fluctuations at the single particle level. In Sec. IV we discuss the role of orientational fluctuations within the lamellae and we address out-of-plane positional fluctuations in Sec. V.

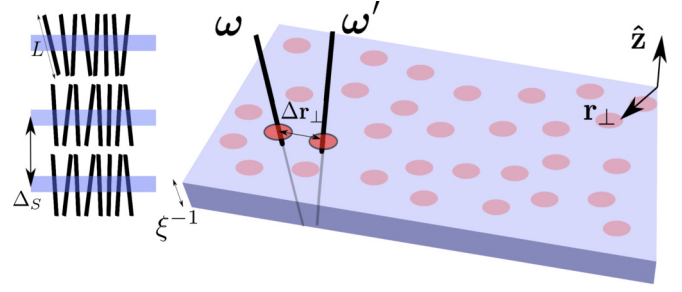


FIG. 1. Left: Sketch of a smectic-A phase of colloidal rods of length  $L$  with layer spacing  $\Delta_s$ . Right: Illustration of the lamellar fluid model. Each lamella is composed of strongly aligned rods with centers of mass (red dots) roughly confined to a narrow slab of width  $\xi^{-1}$  as indicated in blue.

Section VI is devoted to comparing the equation of state of the smectic bulk phase with simulation results. We then move on to discussing the elastic properties in Secs. VII to IX. A comparison with experimental smectics of both lyotropic and thermotropic nature is discussed in Sec. X. Some concluding remarks are formulated in Sec. XI. In the Appendix we test our simplified description of the excluded volume interactions between hard colloidal bodies within a comprehensive bifurcation analysis to identify bulk freezing transitions from a three-dimensional (3D) nematic fluid composed of rod or disk-shaped colloids as well as from a monolayer fluid of rods and compare our predictions against simulation results.

## II. DENSITY FUNCTIONAL THEORY FOR A MONOLAYER ROD FLUID

Let us consider a monolayer fluid consisting of a collection of  $N$  slender rods of length  $L$  and diameter  $D \ll L$  each with their center of mass confined to a 2D  $xy$  plane with area  $A$ . The rods are densely packed at a concentration  $\rho_{\perp} = N/A \sim D^{-2}$  with their main axes aligned along the out-of-plane  $z$  direction (Fig. 1), while each rod experiences weak fluctuations about its average orientation.

The pair interaction  $u_r$  between two rods with long-axis unit vectors  $\omega$  and  $\omega'$  and center-of-mass distance  $\Delta \mathbf{r}$  follows from short-range steric forces,

$$\beta u_r(\Delta \mathbf{r}; \omega, \omega') = \begin{cases} \infty & \Delta \mathbf{r} < \sigma(\Delta \hat{\mathbf{r}}; \omega, \omega') \\ 0 & \text{otherwise} \end{cases}, \quad (1)$$

where  $\beta^{-1} = k_B T$  denotes the thermal energy and  $\sigma$  is the contact distance between the hard cores of the rods which depends nontrivially on the center-of-mass distance unit vector  $\Delta \hat{\mathbf{r}} = \Delta \mathbf{r} / \Delta r$  (for hard spheres  $\sigma$  simply coincides with the sphere diameter).

Next, we apply a second-virial approximation by considering interactions between rod pairs alone. Later we will heuristically account for higher-order virial terms through a simple density rescaling. The grand potential  $\Omega$  for the lamellar fluid can be formally written as follows (dropping the

orientational degrees of freedom for notational convenience),

$$\beta\Omega[\rho] = \int d\mathbf{r}\rho(\mathbf{r})(\ln v\rho(\mathbf{r}) - 1 - \beta\mu) - \frac{1}{2} \int d\mathbf{r}\rho(\mathbf{r}) \int d\mathbf{r}'\rho(\mathbf{r}')\Phi(\Delta\mathbf{r}), \quad (2)$$

with  $\Delta\mathbf{r} = \mathbf{r} - \mathbf{r}'$  and  $\Phi$  the Mayer function that features the pair potential,

$$\Phi(\Delta\mathbf{r}) = e^{-\beta u_r(\Delta\mathbf{r})} - 1. \quad (3)$$

Most importantly,  $\rho(\mathbf{r}) = \rho(\mathbf{r}; \boldsymbol{\omega})$  denotes the one-body rod density while the chemical potential  $\mu$  ensures its proper normalization,  $\int d\mathbf{r} \int d\boldsymbol{\omega} \rho(\mathbf{r}; \boldsymbol{\omega}) = N$ . Finally,  $v$  is the effective thermal volume of each rod which also contains contributions from its rotational momenta. For spherical particles,  $v = \Lambda^3$  with  $\Lambda$  the thermal de Broglie wavelength.

The first term in the free energy Eq. (2) describes the ideal translational and rotational entropy of each rod while the second term relates to the excess free energy that encodes rod-rod correlations at the level of pair interactions. Inside the lamella rod positions are strongly confined around  $z = 0$  while rods are free to move within the lamellar plane ( $xy$ ) that we parametrize by the 2D vector  $\mathbf{r}_\perp$ . The easiest way to constrain the rods to remain in a monolayer configuration would be to introduce an external harmonic potential, e.g.,  $U_{\text{lam}}(z) \propto U_0 z^2$  that would penalize out-of-plane excursions with  $U_{\text{lam}}$  the typical (entropic) energy barrier associated with rods hopping from one layer to the next. Once the smectic potential has been specified one needs to resolve the one-body density  $\rho(\mathbf{r})$  associated with these smectic potentials keeping in mind that this object depends on three positional variables and on two orientational ones.

In this paper we adopt a more manageable strategy by *constraining* the one-body density to take on a simple factorized form,

$$\rho(\mathbf{r}; \boldsymbol{\omega}) = G(z)\rho(\mathbf{r}_\perp; \boldsymbol{\omega}). \quad (4)$$

We invoke a cylindrical coordinate frame  $\mathbf{r} = \mathbf{r}_\perp + z\hat{\mathbf{z}}$  with the planar coordinate denoted by the subscript  $\perp$  and the out-of-plane one by  $z$ . Then  $G$  denotes a Gaussian fluctuation ( $z \in [-\infty, \infty]$ ),

$$G(z) = \left(\frac{\xi}{\pi}\right)^{1/2} \exp(-\xi z^2), \quad (5)$$

where  $(2\xi)^{-1} = \langle z^2 \rangle$  quantifies the mean-squared value for the out-of-plane excursions which are expected to be very small compared to the rod length, i.e.,  $\langle z^2 \rangle \ll L^2$ . Then,  $\lim_{\xi \rightarrow \infty} G_{\xi \rightarrow \infty}$  describes the limiting case of perfectly confined rods. The above parametrization implies that the in-plane positional correlations are coupled to the rod orientations while both are assumed to be unaffected by the out-of-plane rod fluctuations.

Inserting Eq. (4) into the grand potential and minimizing with respect to the unknown planar density  $\rho(\mathbf{r}_\perp; \boldsymbol{\omega})$  we obtain the Euler-Lagrange equation (again dropping all dependencies on  $\boldsymbol{\omega}$  to prevent cluttered notation),

$$\ln v_2\rho(\mathbf{r}_\perp) - \int d\mathbf{r}'_\perp \rho(\mathbf{r}'_\perp)\Phi_{zz}(\Delta\mathbf{r}_\perp) = \beta\mu_\xi, \quad (6)$$

with  $v_n$  denoting the  $n$ -dimensional analog of the thermal volume and  $\Delta\mathbf{r}_\perp = \mathbf{r}'_\perp - \mathbf{r}_\perp$ . We have introduced an intralamellar chemical potential  $\beta\mu_\xi = \beta\mu - \sqrt{\ln(\xi v_1/\pi)} + 1/2$  that is *smaller* than the corresponding value  $\mu$  for the unlayered (isotropic or nematic) bulk fluid. Furthermore,  $\Phi_{zz}(\Delta\mathbf{r}_\perp)$  denotes a Mayer function preaveraged over the out-of-plane fluctuations,

$$\begin{aligned} \Phi_{zz}(\Delta\mathbf{r}_\perp) &= \int_{-\infty}^{\infty} dz G(z) \int_{-\infty}^{\infty} dz' G(z') \Phi(\Delta\mathbf{r}) \\ &= \int_{-\infty}^{\infty} d\Delta z \mathcal{G}(\Delta z) \Phi(\Delta\mathbf{r}), \end{aligned} \quad (7)$$

where the distribution of the out-of-plane differential distance  $\Delta z = z' - z$  is itself a Gaussian,

$$\mathcal{G}(\Delta z) = \left(\frac{\xi}{2\pi}\right)^{1/2} e^{-\frac{1}{2}\xi(\Delta z)^2}. \quad (8)$$

The key ingredient describing the rod interactions in the confined fluid is the second-virial coefficient for two rods with their  $z$  coordinates constrained to a plane,

$$\mathcal{K}_0 = \int d\Delta\mathbf{r}_\perp \Phi_{zz}(\Delta\mathbf{r}_\perp). \quad (9)$$

For purely hard rods,  $\Phi = -1$  if the rod cores overlap and the kernel can be identified with (minus) the excluded volume between two rods with centers of mass confined to a bidimensional plane. This modification aside, the expression above is identical to stationary condition obtained from Onsager theory for conventional hard-rod nematics [13] with  $\rho_\perp(\boldsymbol{\omega}) = \rho_\perp f(\boldsymbol{\omega})$  in terms of some normalized orientational probability  $f(\boldsymbol{\omega})$  that we will specify in Sec. IV. For later reference we also define Fourier transform (FT) of the excluded-volume manifold between two particles,

$$\hat{\mathcal{K}}(\mathbf{q}_\perp) = \int d\Delta\mathbf{r}_\perp \Phi_{zz}(\Delta\mathbf{r}_\perp) e^{i\mathbf{q}_\perp \cdot \Delta\mathbf{r}_\perp}, \quad (10)$$

so that  $\lim_{q_\perp \rightarrow 0} \hat{\mathcal{K}} = \mathcal{K}_0$ . Fortunately, the double convolution of Eq. (7) enables us to recast the kernel as a simple Fourier integral,

$$\hat{\mathcal{K}}(\mathbf{q}_\perp) = \int_{-\infty}^{\infty} \frac{dq_z}{2\pi} [\hat{G}(q_z)]^2 \hat{\Phi}(q_z \hat{\mathbf{z}} + \mathbf{q}_\perp), \quad (11)$$

with  $\hat{G}(q_z) = \exp(-q_z^2/4\xi)$  the FT of the Gaussian probability. Realizing that the Mayer function simply designates (minus) the subvolume where the cores overlap we write,

$$\begin{aligned} \hat{\mathcal{K}}(\mathbf{q}_\perp) &= - \int d\Delta\mathbf{r}_\sigma \int_{-\infty}^{\infty} \frac{dq_z}{2\pi} e^{i\mathbf{q}_\perp \cdot \Delta\mathbf{r}_\sigma - q_z^2/2\xi} \\ &= - \int d\Delta\mathbf{r}_\sigma e^{i\mathbf{q}_\perp \cdot \Delta\mathbf{r}_\sigma} \mathcal{G}(\Delta\mathbf{r}_\sigma \cdot \hat{\mathbf{z}}). \end{aligned} \quad (12)$$

Next we invoke the standard particle-based parametrization of this subvolume via  $\Delta\mathbf{r}_\sigma = \frac{L}{2}t_1\boldsymbol{\omega} + \frac{L}{2}t_2\boldsymbol{\omega}'$  with coordinates  $-1 < t_i < 1$  ( $i = 1, 2$ ). The Jacobian associated with the coordinate transformation is given by  $d\Delta\mathbf{r}_\sigma = \frac{1}{2}L^2 D|\sin\gamma| dt_1 dt_2$  with  $\gamma$  denoting the enclosed angle between the main rod axes. This is our key result that we will elaborate below for two particular situations that are relevant for typical liquid crystal organizations of rod-shaped particles.

### III. TWO LIMITING CASES: NEMATIC AND MONOLAYER FLUID

Two limiting situations are easily identified from Eq. (12). First, if there is *no* lamellar confinement at all, then the rod positions can explore full three-dimensional space such as in a nematic phase. Then  $\mathcal{G} = 1$  and the excluded volume to leading order for sufficiently slender rods  $L/D \gg 1$  can be computed in analytical form [51],

$$\hat{\mathcal{K}}^{(\text{nem})} = -2L^2D |\sin \gamma| j_0\left(\frac{1}{2}\mathbf{q} \cdot \boldsymbol{\omega}\right) j_0\left(\frac{1}{2}\mathbf{q} \cdot \boldsymbol{\omega}'\right) + \mathcal{O}(LD^2), \quad (13)$$

in terms of the spherical Bessel function  $j_0(x) = x^{-1} \sin x$ . Since the focus of our study is not on nematics we do not discuss subsequent contributions of the order of the cylinder volume  $LD^2$  (a technical discussion can be found in Ref. [52]).

The second limiting case is more relevant to a smectic organization and occurs when the rods behave as a strict *monolayer* fluid with no positional fluctuations along the plane normal. The Gaussian distribution then becomes a delta distribution, i.e.,  $\lim_{\xi \rightarrow \infty} \mathcal{G} = \delta(\Delta \mathbf{r}_\sigma \cdot \hat{\mathbf{z}})$ . The hard-core kernel  $\hat{\mathcal{K}}_c(\mathbf{q}_\perp)$  is then equivalent to the FT of the *excluded area* between two rods at equiplanar centers of mass ( $\Delta z = 0$ ). This quantity has been analyzed in detail by Poniewierski [51]. Equating  $\mathcal{G} = \delta(\Delta \mathbf{r}_\sigma \cdot \hat{\mathbf{z}})$  in Eq. (12) we find,

$$\begin{aligned} \hat{\mathcal{K}}^{(\text{mono})} &= -\frac{L^2D}{2} |\sin \gamma| \prod_{i=1}^2 \int_{-1}^1 dt_i \delta(\Delta \mathbf{r}_\sigma \cdot \hat{\mathbf{z}}) e^{i\mathbf{q}_\perp \cdot \Delta \mathbf{r}_\sigma} \\ &= -L^2D |\sin \gamma| \frac{\sin(R/m)}{R} + \mathcal{O}(D^2), \end{aligned} \quad (14)$$

where  $R$  is a length scale compiling the coupling between the wave vector and rod orientations,

$$R = b_z(\mathbf{q}_\perp \cdot \mathbf{a}) - a_z(\mathbf{q}_\perp \cdot \mathbf{b}), \quad (15)$$

and  $\mathbf{a} = L\boldsymbol{\omega}/2$ ,  $\mathbf{b} = L\boldsymbol{\omega}'/2$ ,  $a_z = |\mathbf{a} \cdot \hat{\mathbf{z}}|$ , and  $b_z = |\mathbf{b} \cdot \hat{\mathbf{z}}|$ . The length  $m$  selects the maximum of the latter two rod projections onto the lamellar normal  $\hat{\mathbf{z}}$  in terms of the Heaviside step function  $\Theta$ ,

$$m = a_z \Theta(a_z - b_z) + b_z \Theta(b_z - a_z). \quad (16)$$

The first contribution in Eq. (14) is of order  $\mathcal{O}(LD)$  and vanishes for a pair of perfectly parallel cylinders ( $\gamma \rightarrow 0$ ). The next order term should be of  $\mathcal{O}(D^2)$ , which we approximate here by the FT of a disk with radius  $D$ . We thus obtain a simplified expression for the total kernel for a monolayer rod fluid,

$$\hat{\mathcal{K}}^{(\text{mono})} \sim -L^2D |\sin \gamma| \frac{\sin(R/m)}{R} - \pi D^2 \frac{J_1(q_\perp D)}{\frac{1}{2}q_\perp D}, \quad (17)$$

with  $J_1$  a Bessel function of the first kind. At present, there is no exact expression for the  $\mathcal{O}(D^2)$  term which should depend on the orientation of both rods and involve subtle correlations between the cylinder ends [52]. We remark that the excluded volume for infinitely thin rods ( $L/D \rightarrow \infty$ ), given by the zero-wave-number limit of Eq. (17), is identical to the one derived by Oettel *et al.* [53]. In real smectic phases, however, the rods are never perfectly confined to the lamellar midplane but are able to exercise small out-of-plane excursions that we will describe in Sec. V.

In the Appendix we demonstrate that our approach to describing excluded-volume interactions, namely pairing an orientationally dependent contribution for infinitely thin particles with a tractable parallel core term, can be applied to both rods and disks alike and allows us to accurately predict the onset of smectic or columnar freezing from a nematic reference fluid as well as the fluid-solid transition within a single smectic monolayer.

### IV. ORIENTATIONAL FLUCTUATIONS

We focus on the smectic-A phase in which there is no long-ranged positional order transverse to the nematic director and the one-body density can be written as  $\rho_\perp(\boldsymbol{\omega}) = \rho_\perp f(\boldsymbol{\omega})$  in terms of a fixed planar rod density  $\rho_\perp$ . For simplicity, we use the monolayer expression for the excluded volume Eq. (14) and introduce the Helmholtz free energy of a lamellar fluid ignoring any term that is independent of the orientational probability  $f$ ,

$$\frac{\beta F_L}{N} \sim \langle \ln f(\boldsymbol{\omega}) \rangle + \frac{8\ell}{\pi} \phi_\perp g(\phi_\perp) \left\langle \left\langle \frac{|\sin \gamma|}{\bar{m}} \right\rangle \right\rangle. \quad (18)$$

The brackets are short-hand for the angular integral  $\langle \cdot \rangle = \int d\boldsymbol{\omega} f(\boldsymbol{\omega})$  and likewise for a double angular average  $\langle \langle \cdot \rangle \rangle = \int d\boldsymbol{\omega} f(\boldsymbol{\omega}) \int d\boldsymbol{\omega}' f(\boldsymbol{\omega}')$ . We further introduced the normalized lengths  $\bar{m}(\boldsymbol{\omega}, \boldsymbol{\omega}') = m/(L/2)$ , planar rod packing fraction  $\phi_\perp = (\pi/4)\rho_\perp D^2$ , and rod aspect-ratio  $\ell = L/D \gg 1$ . Since the fluid residing within each lamella is spatially uniform, we apply a Lee-Parsons rescaling of the packing fraction  $\phi_\perp \rightarrow \phi_\perp g(\phi_\perp)$ , where  $g(\phi) = (1 - \frac{3}{4}\phi)/(1 - \phi)^2$  represents a correction factor to the second-virial approach, derived from the Carnahan-Starling equation of state for hard spherical particles, that entails an *ad hoc* resummation of higher-order virial terms [54,55]. Despite the heuristic nature of the theory, the Lee-Parsons formalism is known to give quantitatively reliable results for the fluid phase behavior of elongated hard cylinders at elevated packing conditions [17]. We remark that the free energy above is very similar to that of a nematic phase except for the factor  $\bar{m}$  which, as we will argue, will be very close to unity if the orientational fluctuations are weak. A crucial difference with the nematic fluid with prescribed density  $\rho_{\text{nem}}$ , however, is that the planar packing fraction  $\phi_\perp$  is not *a priori* known but is controlled by the smectic spacing for a given overall (3D) rod packing fraction as we will point out in Sec. VI.

The formal way forward is to resolve the Euler-Lagrange equation from the extremum condition  $\delta F/\delta f = 0$  which can be done numerically [56,57]. In this study, we will pursue a much simpler algebraic route to addressing intralamellar orientational order by assuming orientational order to be both asymptotically strong and of simple uniaxial symmetry so that the angular probability only depends on the polar angle  $\theta$  between the rod orientation vector  $\boldsymbol{\omega}$  and the layer normal along the  $z$  axis. Both criteria should be fulfilled for stable smectic structures composed of uniaxial rods whose interactions are apolar and achiral. Then  $f(\theta)$  can be approximated by a Gaussian trial function [58],

$$f_G(\boldsymbol{\omega}) \sim \frac{\alpha_\perp}{4\pi} e^{-\frac{1}{2}\alpha_\perp \theta^2}, \quad (19)$$

which applies within the interval  $0 < \theta < \pi/2$  combined with its mirror form  $f(\pi - \theta)$  for  $\pi/2 < \theta < \pi$  and  $\alpha_\perp \gg 1$  a variational parameter that is required to be large for consistency reasons given that the Gaussian trial form does not reduce to the required isotropic distribution  $f_G = (4\pi)^{-1}$  in the limit  $\alpha_\perp \rightarrow 0$ . In a dense smectic environment, rod alignment is usually very strong and this criterion is readily met. Ignoring constant terms we write the Helmholtz free energy as a combination of orientational and excluded-volume entropy per particle and keep only leading-order terms valid for small interrod angles. Then  $\bar{m} \rightarrow 1$  and the free energy Eq. (18) takes the following form,

$$\frac{F_L}{N} \sim \langle \ln f_G(\theta) \rangle + 4 \frac{\ell}{\pi} \phi_\perp g(\phi_\perp) \langle \langle \gamma \rangle \rangle. \quad (20)$$

The double orientational averages are known up to leading order for large  $\alpha_\perp$  [9,58],

$$\begin{aligned} \langle \ln f_G(\theta) \rangle &\sim \ln \alpha_\perp - 1 \\ \langle \langle \gamma \rangle \rangle &\sim \sqrt{\pi/\alpha_\perp}. \end{aligned} \quad (21)$$

Minimizing the lamellar free energy  $F_L$  with respect to  $\alpha_\perp$  then yields a quadratic relation with the planar rod packing fraction,

$$\alpha_\perp \sim 4(\phi_\perp g(\phi_\perp) \ell)^2 / \pi, \quad (22)$$

similar to the case of a nematic fluid.

## V. OUT-OF-PLANE FLUCTUATIONS

We will now release the constraint of infinite lamellar confinement (monolayer case) and consider the density distribution  $\rho(\mathbf{r}) = \rho_\perp p(z)$  with intralamellar density  $\rho_\perp$  and out-of-plane positional fluctuations along the layer normal described by a probability  $p(z)$ . Each rod is able to explore the full range of  $z$  positions, subject to the constraint that the rod must not overlap with a neighboring particle whose mass center resides in the adjacent smectic layer a distance  $\Delta_S$  away from the test rod. For simplicity, we assume the rods to be parallel and coaxial so that overlap occurs whenever  $|\Delta z| < L$ . We only consider nearest neighbor lamellar interactions. Then we may construct a fluctuation free energy per rod that depends on a single positional degree and reflects a balance between translational entropy and a volume-exclusion penalty,

$$\begin{aligned} \frac{\beta \mathcal{F}_{\text{fluc}}}{N} &= \int_{-\infty}^{\infty} dz p(z) [\ln \{\Lambda p(z)\} - 1] + \frac{1}{2} \int_{-\infty}^{\infty} dz p(z) \\ &\times \int_{-\infty}^{\infty} dz' \{p(z' - \Delta_S) + p(z' + \Delta_S)\} \Theta(L - |\Delta z|), \end{aligned} \quad (23)$$

with  $\Lambda$  the thermal wavelength. The corresponding single-particle distribution  $p(z)$  can be resolved self-consistently

through formal minimization  $\delta \mathcal{F}_{\text{fluc}}[p]/\delta p = 0$  which leads to,

$$\begin{aligned} p(z) &= \exp \left( \lambda' - \int_{-\infty}^{\infty} dz' p(z') \{H(L - |\Delta z - \Delta_S|) \right. \\ &\quad \left. + H(L - |\Delta z + \Delta_S|) \} \right), \end{aligned} \quad (24)$$

where  $\lambda'$  denotes a multiplier ensuring normalization  $\int dz p(z) = 1$ . If we assume the rods in the neighboring lamellae to be fixed at their midplane, then we can establish an analytical mean-field solution from  $p(z') \approx \delta(0)$  which gives  $p(z) = 1/2(\Delta_S - L)$  for  $|z| < (\Delta_S - L)$  and  $p(z) = 0$  otherwise. A numerical solution for  $p(z)$  can be obtained through iteration but the results merely lead to entropic rounding at the edges of the step function thus rendering the distribution continuously differentiable. Even though  $p(z)$  is not Gaussian, we may tentatively identify  $p(z) = G(z)$  via Eq. (5) and connect the mean-squared out-of-plane displacement to the Gaussian parameter  $\xi$ ,

$$\xi \sim \frac{3}{2(\Delta_S - L)^2}, \quad (25)$$

revealing, as expected, that out-of-plane fluctuations  $\sim \xi^{-1}$  grow stronger at larger lamellar distances  $\Delta_S > L$ .

For real smectic phases such as those composed of *fd* rods, the out-of-plane fluctuations and the typical energy barrier the rods need to jump from one layer to the next have been studied in detail [23,44,45,59]. The density distribution normal to the layer for small deviations from the lamellar midplane can be described by a Gaussian,

$$p(z) \approx \exp[-2\pi^2 U_0 (z/L)^2] \quad z/L \ll 1, \quad (26)$$

with  $U_0$  a typical smectic layer potential (expressed in units  $k_B T$ ) for which experimental values are available. It should be noted that the non-Gaussian tail of  $p(z)$  plays an essential role in determining the potential amplitude. Comparing with our Gaussian distribution we may identify the smectic potential to the layer spacing for small out-of-plane excursions  $z/L \ll 1$ ,

$$U_0 \sim \frac{3}{4\pi^2} \left( \frac{\Delta_S}{L} - 1 \right)^{-2}. \quad (27)$$

In Sec. X we will discuss a comparison with experimental measurements of the smectic potential for *fd* rods.

### A. Effect of layer interdigitation

The naive description proposed so far overestimates the smectic potential since rods are known to migrate from one layer to the next [44,45] which suggests a degree of *dynamic interdigitation* between smectic layers. This can be understood from the fact that rods are never closely packed together within each lamella but experience a certain degree of free volume that enables particles to at least partially penetrate into a neighbor layer. Clearly, interdigitation becomes less prominent at larger packing conditions. This effect can be taken into account, at a simplified mean-field level, by introducing a finite layer interdigitation potential  $W$  which broadens the out-of-plane distribution  $p(z)$  and partly captures the non-Gaussian tails of the out-of-plane distribution which

now reads,

$$p(z) = \begin{cases} 1 & |z| < \Delta_S - L \\ e^{-\beta W} & \Delta_S - L < |z| < \Delta_S - L + \zeta, \\ 0 & |z| > \Delta_S - L + \zeta \end{cases} \quad (28)$$

with  $0 < \zeta < L$  a interdigitation depth such that  $\zeta = L$  implies that each rod can fully penetrate the adjacent layer while for  $\zeta = 0$  no interdigitation occurs at all and the previous result Eq. (24) is recovered. In real systems with strong in-plane crowding, we expect  $\zeta$  to be only a fraction of the rod length. After some algebra, we find that the smectic layer potential associated with  $p(z)$  reads,

$$U_0 \sim \frac{3[(\bar{\Delta}_S - 1) + e^{-\beta W} \bar{\zeta}]}{4\pi^2\{(\bar{\Delta}_S - 1)^3 + e^{-\beta W}[(\bar{\Delta}_S - 1 + \bar{\zeta})^3 - (\bar{\Delta}_S - 1)^3]\}}, \quad (29)$$

in terms of the interdigitation depth  $\bar{\zeta} = \zeta/L$  and spacing  $\bar{\Delta}_S = \Delta_S/L$  both normalized to the rod length. The insertion potential can be interpreted as a potential of mean force represented by the free energy cost of inserting a rod into a bidimensional fluid for which scaled particle theory (SPT) can be invoked [60,61]. Then  $W$  is simply the excess chemical potential  $\mu_{\text{ex}}$  of a bidimensional fluid of hard disks representing the rod cross sections residing on the lamellar area  $A$ . This expression is well known and reads [62],

$$\beta W = -\ln(1 - \phi_{\perp}) + \frac{1 + \phi_{\perp}(1 - \phi_{\perp})}{(1 - \phi_{\perp})^2}, \quad (30)$$

where  $\phi_{\perp}$  denotes the in-plane packing fraction that implicitly depends on the lamellar spacing via  $\phi_{\perp} = \phi \Delta_S$ . In fact, the SPT theory and variations thereof [63] have been used routinely in cell-type theories for smectic and other liquid crystal states [38–42]. The presence of layer interdigitation lowers the smectic potential to values that are in good agreement with experimental measurements on smectic phases of *fd* rods as we will discuss in Sec. X.

## VI. FROM MONOLAYER FLUID TO SMECTIC LIQUID CRYSTAL

We now wish to construct a tractable thermodynamic theory for a 3D smectic phase composed of  $M \rightarrow \infty$  lamellae. For purely hard interactions an appealing route is to use cell theory to correlate the 2D fluid behavior with a 1D periodicity of the smectic liquid crystal.

The basic assumption of the cell approach for describing a smectic structure is that the vertical degrees of each rod (along the layer normal) are constrained by the presence of the adjacent smectic layers such that rods are not permitted to cross layer boundaries. Maximum positional freedom of each rod is then dictated by the size of the cell which is proportional to the smectic layer spacing. With these constraints, the 1D ordered dimension and the 2D fluid dimensions of the smectic structure are fully decoupled and can be modelled separately. Similar arguments can be applied to other positionally ordered liquid crystals, such as the columnar, and even solids [38]. Focusing on the 1D ordered dimension, we assume that the layers impart some effective potential that can be purely hard-core like [38,39] or feature an additional continuous potential

to account for long-range repulsive interactions between particles [64,65]. Then the excess free energy is connected to the mean out-of-plane free distance  $\Delta_S$  each rod is able to explore before touching a rod from an adjacent layer. The configurational integral of a collection of  $M$  uncorrelated cells reads [66],

$$Q \approx \left( \Lambda^{-1} \int dz e^{-\beta u_{\text{cell}}} \right)^M, \quad (31)$$

where the cell potential can be reverse-engineered from the out-of-plane-fluctuation probability Eq. (28) through a simple Boltzmann inversion  $u_{\text{cell}}(z) = -\beta^{-1} \ln p(z)$ ,

$$u_{\text{cell}}(z) = \begin{cases} 0 & |z| < \Delta_S - L \\ W & \Delta_S - L < |z| < \Delta_S - L + \zeta. \\ \infty & |z| > \Delta_S - L + \zeta \end{cases} \quad (32)$$

The soft potential  $W$  accounts, albeit heuristically, for the degree of rod interdigitation across adjacent lamellae. The excess free energy per rod  $\beta F_{\text{cell}} = -\ln Q$  associated with smectic layering in the thermodynamic limit  $M \rightarrow \infty$  thus reads,

$$\frac{F_{\text{cell}}}{N} \sim -\ln[\Lambda^{-1}(\Delta_S - L + \zeta e^{-\beta W})] - \ln 2. \quad (33)$$

The contribution proportional to the interdigitation depth  $\zeta$  is due to the *soft-cell* potential Eq. (32) and is not considered in conventional cell approaches where this effect is ignored, i.e.,  $W \rightarrow \infty$  ( $\zeta = 0$ ). Conservation of number of particles and the single-occupancy condition (each rod belongs to only one smectic layer) requires that the overall (3D) rod density relate to the in-plane concentration via  $\rho = \rho_{\perp}/\Delta_S$ .

We now wish to put our model to a quantitative test by comparing the equation of state of the (3D) smectic phase for hard cylinders to results from computer simulation for hard spherocylinders. Subtle end-cap effects that distinguish these two particle shapes are deemed of minor importance for sufficiently elongated particles  $L/D \gg 1$ . In order to address the thermodynamics of the smectic phase we combine the above cell contribution with the intralamellar fluid contribution discussed previously [cf. Eq. (18)]. Ignoring all constant factors we find a simple expression that incorporates the ideal, orientational, rod excluded-volume, and lamellar entropies, respectively,

$$\begin{aligned} \frac{F_S}{N} &\sim \ln \phi + 2 \ln[\phi_{\perp} g(\phi_{\perp})] + 2\phi_{\perp} g(\phi_{\perp}) \\ &\quad - \ln \left[ 1 - \bar{\Delta}_S^{-1} (1 - \bar{\zeta} e^{-\beta W}) \right], \end{aligned} \quad (34)$$

where  $\bar{\Delta}_S = 2\pi/q_S L$  denotes the spacing (in units rod length) between adjacent smectic layers. In the Gaussian approximation, the orientation-dependent part of the excluded volume produces a constant of “2” as originally pointed out by Odijk [67]. The equilibrium spacing is then easily found from minimization  $\partial F_S/\partial \Delta_S = 0$  and the pressure from  $P_S = \phi^2[\partial(F_S/N)/\partial \phi]$ . The results in Fig. 2 demonstrate that our simple model gives a quantitatively reliable prediction of the equation of state at relatively low packing fraction ( $\phi < 0.5$ ) while somewhat overestimating the simulated values at large packing fraction. We find that the pressure is rather insensitive to the choice of the interdigitation depth  $\zeta$ . This confirms the

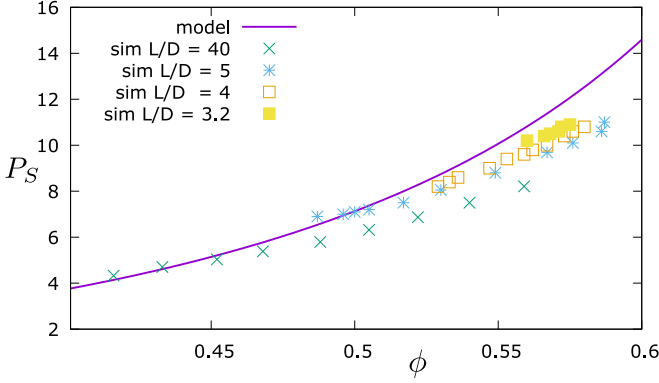


FIG. 2. Equation of state of a smectic-A phase of hard rods. Plotted is the osmotic pressure  $P_S$  (in units  $k_B T$  per rod volume) versus the packing fraction  $\phi$ . The prediction from the theoretical model is generic and does not depend on the rod aspect ratio  $\ell = L/D$ . Simulation results are quoted from McGrother *et al.* [17] ( $L/D = 3.2, 4, 5$ ) and Bolhuis *et al.* [18] ( $L/D = 40$ ).

robustness of the cell description in the sense that the thermodynamic properties of the smectic phase are insensitive to the details of the cell potential. However, we will demonstrate in the next section that the mechanical properties of the smectic material *do* depend on the out-of-plane fluctuations which in turn are steered by the degree of layer interdigitation and the choice of  $u_{\text{cell}}$ .

## VII. LAYER COMPRESSION MODULUS

In order to describe long-wavelength elastic distortions of a colloid-based smectic material we consider the elastic free energy per unit volume of a smectic liquid crystal which is given by the following expression [1],

$$\frac{F_S}{V} = \frac{B}{2} \left[ \frac{\partial u}{\partial z} - \frac{1}{2} \left( \frac{\partial u}{\partial x} \right)^2 \right]^2 + \frac{K_1}{2} \left( \frac{\partial^2 u}{\partial x^2} \right)^2, \quad (35)$$

with  $u(x, z)$  the displacement field denoting a local displacement of the smectic layer away from its equilibrium position. The deformations are described by two elastic moduli; the layer compression modulus  $B$  and splay modulus  $K_1$ . The latter is associated with layer bending which in the above expression is assumed to be unidirectional along the  $x$  axis (see Fig. 4). Both moduli can be combined into a single length scale; the smectic penetration length  $\lambda = \sqrt{K_1/B}$ . Furthermore, the Landau-Peierls instability dictates that the mean-squared fluctuations of the displacement field  $u$  diverge with the system size  $\ell_s$  [1,8],

$$\langle u(\mathbf{r})^2 \rangle = \frac{k_B T}{8\pi \sqrt{K_1 B}} \ln(\ell_s / \Delta_S), \quad (36)$$

with  $\sqrt{K_1 B}$  a characteristic energy scale per unit area which along  $\lambda$  defines the elastic response of a smectic material. We now wish to quantify these for the specific case of a hard-rod smectic by analyzing each of the contributions separately. First, the compression modulus  $B$  can be defined following a general analysis of Ref. [68] for bilayer smectics

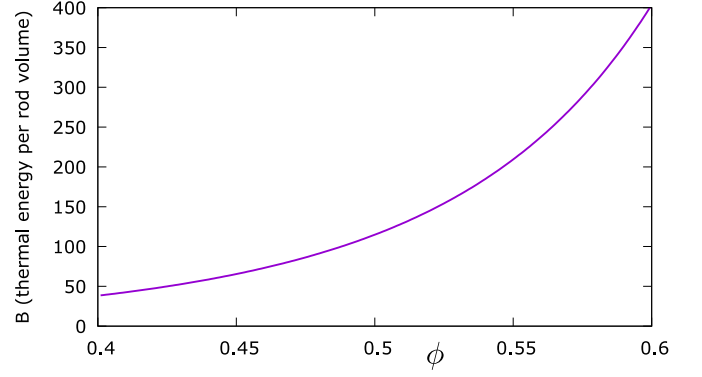


FIG. 3. Layer compressibility modulus  $B$  of a hard-rod smectic as a function of the overall packing fraction  $\phi$ . The modulus is expressed in units  $k_B T / v_r$  in terms of the rod volume  $v_r = \frac{\pi}{4} LD^2$ .

with spacing  $\delta_S$ ,

$$B = \delta_S \left( \frac{\partial^2 f_L}{\partial \bar{\delta}_S^2} \right)_\mu, \quad (37)$$

with  $\bar{\delta} = \delta_S - h$  and  $h$  the bilayer thickness. The free energy  $f_L$  per bilayer and unit area must be defined at constant chemical potential of the bilayer constituents in order to facilitate fluctuations in the surface coverage on dilation or compression of the smectic layers. Translating this expression to our current entropy-stabilized hard-rod smectic with spacing over rod length  $\bar{\Delta}_S$  we find that the layer compressibility modulus (rendered dimensionless in units of thermal energy  $k_B T$  per particle volume  $v_r$ ) reads,

$$B = \bar{\Delta}_S \left( \frac{\partial^2 [\phi_\perp F_S / N]}{\partial \bar{\Delta}_S^2} \right)_\phi. \quad (38)$$

The difference with the previous definition for the bilayer case is that layer compression happens at *constant* overall rod packing fraction instead of chemical potential and that the average layer thickness is fixed at  $L$ . This seems a reasonable assumption for most smectic organizations, including bilayer phases. Our prediction of the compressibility modulus is shown in Fig. 3 and features a fairly steep (about fourfold) increase of the compression resistance of a hard-rod smectic at moderately high densities  $0.4 < \phi < 0.55$ .

## VIII. SPLAY MODULUS

The modulus  $K_1$  refers to a splay deformation of the layer normal, which coincides with the orientational director of the rods, on layer bending. To the best of our knowledge, no attempt has been made so far to quantify  $K_1$  from microscopic theory. For *nematic* phases, however, theoretical predictions of the Frank elastic moduli have been proposed decades ago starting with the work of Straley [69]. Within the second-virial approximation the splay modulus is formally given by the following expression [10,69],

$$K_1 = k_B T \frac{\rho^2}{2} g(\phi) \left\langle \left\langle \int d\mathbf{r} (\Delta x)^2 \Phi(\Delta \mathbf{r}) \omega_x \omega'_x \right\rangle \right\rangle_f, \quad (39)$$

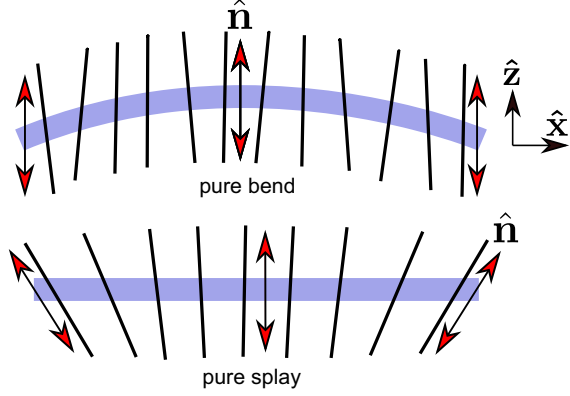


FIG. 4. Two principal effects of layer bending; (top) a pure bend deformation of the smectic layer keeping a uniform (splayless) director field and (bottom) a splay deformation of the director field without layer bending. The lamellar midplane is indicated in blue.

with  $\dot{f}$  denoting the derivative of the orientation distribution with respect to its argument. Using an asymptotic expansion based on the trial form Eq. (19) Odijk [70] obtained the following scaling expression, valid in the limit of strong nematic alignment,

$$\beta K_1 D \sim \frac{7}{8\pi} \phi \ell, \quad (40)$$

with  $\ell = L/D$  the rod aspect ratio. In the smectic phase, the rod positions are not uniformly distributed but strongly localized about the lamellar midplane. The corresponding microscopic expression for the splay modulus of a smectic phase reads,

$$\begin{aligned} \beta K_1 &\sim \frac{\rho^2}{2} g(\phi_\perp) \Delta_S \left\langle \left\langle \int d\mathbf{r}_\perp (\Delta x)^2 \Phi_{zz} \omega_x \omega'_x \right\rangle \right\rangle_f \\ &\sim -\frac{\rho^2}{2} g(\phi_\perp) \Delta_S \left\langle \left\langle \int d\mathbf{r}_\sigma \mathcal{G}(\Delta z_\sigma) (\Delta x_\sigma)^2 \omega_x \omega'_x \right\rangle \right\rangle_f. \end{aligned} \quad (41)$$

Analogous to the case of a nematic phase we may obtain a scaling expression of the double orientational average using the Gaussian algebraic manipulations outlined in Ref. [70]. The key step is to eliminate the azimuthal part  $\cos 2\Delta\varphi = 2\cos^2 \Delta\varphi - 1$  via  $\gamma^2 \sim \theta^2 + \theta'^2 - 2\theta\theta' \cos \Delta\varphi$  and apply double Gaussian averages over the remaining combinations of  $\gamma$  and  $\theta_1$  and  $\theta_2$  that are listed in Ref. [70]. A tedious but straightforward computation then leads to following result up to leading order for weak out-of-plane fluctuations ( $\xi L^2 \gg 1$ ),

$$\beta K_1 D \sim \frac{11}{2\pi^{3/2}} \alpha_\perp^{-1/2} (\phi \ell)^2 g(\phi_\perp) \left( 1 - \frac{6}{\sqrt{2\pi} \xi L^2} \right). \quad (42)$$

Higher-order corrections are of  $\mathcal{O}(\xi^{-1})$  and will not be considered here. Plugging in the quadratic relationship for  $\alpha_\perp$  [Eq. (22)] we obtain the following analytical result,

$$\beta K_1 D \sim \frac{11}{4\pi} \left( 1 - \frac{6}{\sqrt{2\pi} \xi L^2} \right) \phi \ell. \quad (43)$$

We infer from comparison with Eq. (40) that in the absence of positional fluctuations ( $\xi \rightarrow \infty$ ) the splay elasticity is about

three times larger than that of a nematic phase at comparable rod concentration  $\phi \ell$ . As expected, the presence of out-of-plane fluctuations with strength  $\xi^{-1}$  reduces the splay modulus and will only reach the nematic level for very weakly ordered smectics with a large spacing and strong positional fluctuation about the lamellar midplane. For a typical hard-rod smectic with a spacing of about  $\Delta_S = 1.1L$ , equivalent to  $\xi L^2 \sim \mathcal{O}(10^2)$ ,  $K_1$  is about 15% smaller than in the limit of infinite lamellar confinement ( $\xi \rightarrow \infty$ ).

So far we have only considered pure splay and ignored any bending of the layers. Let us now contemplate an infinitesimal bending of the smectic layer while keeping a *uniform* director field  $\hat{\mathbf{n}}(\mathbf{r}) = \hat{\mathbf{z}}$ . This amounts to bending a smectic layer without splaying the director field as illustrated in Fig. 4. The excluded volume Eq. (14) between two test rods with centers of mass confined on a weakly curved 2D plane now depends on the curvature  $\kappa$  which should be weak on the scale of the particle size ( $\kappa L \ll 1$ ). The projected excluded volume (with dimension area) between two thin hard rods with centers of mass residing on a curved (2D) layer is given by minus the kernel  $\mathcal{K}$  and reads,

$$\begin{aligned} \mathcal{K}(\kappa) &\sim -\frac{1}{2} L^2 D |\sin \gamma| \prod_{i=1}^2 \int_{-1}^1 dt_i \\ &\times \mathcal{G}\{\Delta z_\sigma - \kappa^{-1} [\sqrt{1 - (\kappa \Delta x_\sigma)^2} - 1]\}. \end{aligned} \quad (44)$$

Taylor expanding up to second order in the curvature  $\kappa$  formally gives,

$$\mathcal{K}(\kappa) \approx \mathcal{K}(0) + \kappa^2 \delta \mathcal{K} + \mathcal{O}(\kappa^4). \quad (45)$$

We are primarily interested in the correction  $\delta \mathcal{K}$  which has dimension length to the fourth power. The double integral Eq. (44) can be rendered analytically tractable by keeping the lowest-order term for small angular fluctuations  $\theta \ll 1$  and positional fluctuations about the smectic plane  $\xi L^2 \gg 1$  we find,

$$\delta \mathcal{K} \sim \frac{3}{128\sqrt{2\pi}} L^5 D \xi |\gamma|^5. \quad (46)$$

The elastic free energy density corresponds to the change in free energy per unit volume incurred by slight layer bending. Within the second-virial approximation it can be written as,

$$\frac{\delta F_S}{V} \approx \frac{1}{2} k_B T \rho^2 g(\phi_\perp) \Delta_S \langle \langle -\delta \mathcal{K} \rangle \rangle \kappa^2. \quad (47)$$

The brackets denote a double average over the orientational distribution function which we assume is unaltered by layer bending. We may read off the bend modulus under the constraint of a uniform director field,

$$K_b \sim k_B T \rho^2 g(\phi_\perp) \Delta_S \langle \langle -\delta \mathcal{K} \rangle \rangle. \quad (48)$$

It is easily ascertained that this quantity has units of force. Using the Gaussian orientational average  $\langle \langle |\gamma|^5 \rangle \rangle \sim 60\pi^{1/2} \alpha_\perp^{-5/2}$  [70] up to leading order for strong in-plane alignment  $\alpha_\perp \gg 1$  combined with Eq. (22) we find the following scaling expression for the bend modulus,

$$\begin{aligned} \beta K_b D &\propto -(\xi L^2) \alpha_\perp^{-5/2} \\ &\propto -(\phi \ell)^{-3} g(\phi_\perp)^{-4} \Delta_S^{-4} (\xi L^2). \end{aligned} \quad (49)$$



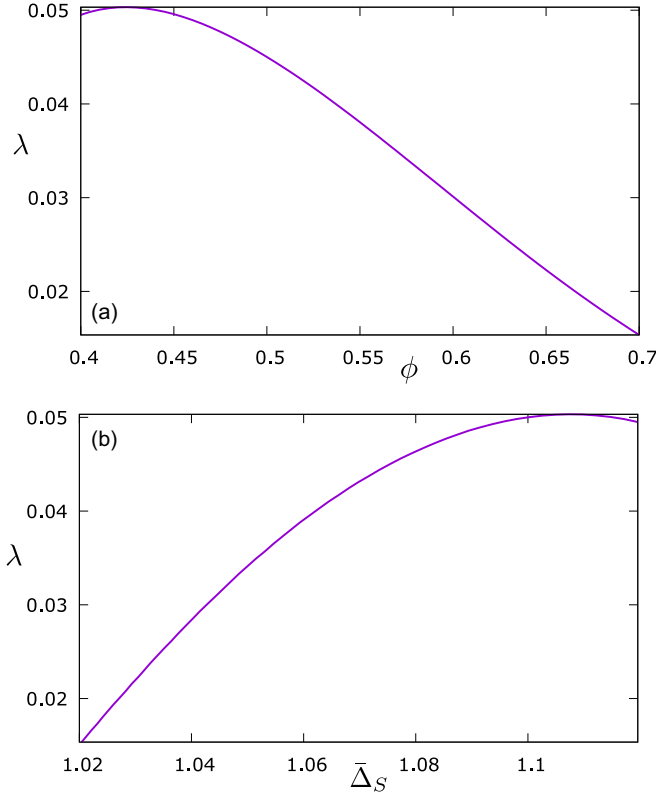


FIG. 5. (a) Penetration length  $\lambda = \sqrt{K_1/B}$  of a hard-rod smectic in units of the rod length  $L$  versus the rod packing fraction  $\phi$ . The penetration length is shape-independent and does not depend on the rod aspect ratio. (b) Same as a function of the smectic layer spacing  $\bar{\Delta}_S$  (in units rod length  $L$ ).

We observe that the layer stiffness is much more sensitive to the strength of the orientational fluctuations  $\alpha_\perp$  than to the out-of-plane fluctuations which are principally controlled by the lamellar distance  $\Delta_S$  via Eq. (25). Noting that  $\phi\ell \gg 1$  for thermodynamically stable smectics and  $\xi L^2 \sim \mathcal{O}(10^2)$  for typical lamellar spacings we find that for moderate rod aspect ratio  $\ell = 10$  the bend contribution is at least two orders of magnitude smaller much than the splay modulus Eq. (43). The difference is even greater for slender rods  $\ell \gg 10$  where splayless layer bending has a marginal effect on the smectoe-elastic response. We remark that  $K_1$  depends nontrivially on the packing fraction because the equilibrium spacing  $\Delta_S$  itself depends nonanalytically on  $\phi$  though the minimum condition  $\partial F_S/\partial \bar{\Delta}_S = 0$  of the smectic free energy Eq. (34).

Now that we have established that director splay is much more important than pure layer bending, at least for hard-rod smectics, we may combine the prediction for the compressibility modulus  $B$  with the expression for the intralamellar splay elastic constant Eq. (43) and compute the smectic penetration length  $\lambda = \sqrt{K_1/B}$  shown in Fig. 5. We find that this length constitutes only a tiny fraction of the rod length (or smectic layer spacing) and that it decreases linearly at elevated packing conditions. We further observe that the penetration length exhibits a (weak) maximum around  $\phi \approx 0.43$ . We have not verified the robustness of the maximum in relation to the approximations made in our theory.

## IX. ROLE OF BACKBONE FLEXIBILITY

In order to render our theory more appropriate for experimental systems such as filamentous virus *fd* rods we have to account for the slight flexibility of the virus backbone, which has been shown to quantitatively affect the phase diagram [71,72]. Liquid crystals of semiflexible polymers have also been the subject of recent simulations in an effort to test scaling concepts that were put forward in earlier theoretical work on polymeric liquid crystals (see Refs. [73,74] for a discussion).

In our theory we shall account for backbone flexibility by introducing a correction to the orientational entropy of perfectly rigid rods considered thus far in our modeling. The presence of rod flexibility, however slight, gives rise to an additional entropy generated by the internal configurations of a so-called wormlike chain (wlc) [9] which can be described by the following nonlinear expression in the orientational probability  $f$  [75,76],

$$\frac{F_{\text{wlc}}}{N} = -\frac{2L}{3\ell_p} \int d\omega [f(\omega)]^{1/2} \nabla^2 [f(\omega)]^{1/2}. \quad (50)$$

Here  $\nabla^2$  denotes the Laplace operator on the unit sphere and  $\ell_p$  is the persistence length that represents the typical length scale over which the orientational fluctuations of the local (Kuhn) segments of each rod are correlated. Since *fd* rods are rather stiff with a persistence length strongly exceeding the contour length ( $\ell_p \sim 3 - 10L$ ) [71], the entropy associated with the internal fluctuations of the effective segments is relatively small compared to the orientational entropy of the entire rod. In the semiflexible regime ( $D \ll \ell_p \ll L$ ) it can be demonstrated that the second-virial coefficient between two wormlike chains between is the same as the one for rigid rods [9,58]. Strictly, this is no longer the case in the rod limit  $\ell_p \gg L$  where rod-rod exclusion is expected to depend on the degree of flexibility but we shall assume deviations from the rigid rod excluded volume to be small for the case of *fd*.

The wormlike chain entropy can be estimated from the Gaussian orientational distribution  $f_G$  and reads up to leading order for strong orientational order [9],

$$\int d\omega [f_G(\omega)]^{1/2} \nabla^2 [f_G(\omega)]^{1/2} \sim -\frac{\alpha_\perp}{2}. \quad (51)$$

From which we obtain,

$$\frac{F_{\text{wlc}}}{N} \sim \frac{L\alpha_\perp}{3\ell_p}. \quad (52)$$

In case of strong in-plane orientation order ( $\alpha_\perp \gg 1$ ) the number of polymer conformations is severely limited which thus leads to a free energy penalty. Adding the wormlike chain correction to the Helmholtz free energy per particle Eq. (20) for the lamellar fluid we find (ignoring irrelevant constants),

$$\frac{F_L}{N} \sim \ln \alpha_\perp + 4\frac{\ell}{\pi} \phi_\perp g(\phi_\perp) \sqrt{\pi/\alpha_\perp} + \frac{L\alpha_\perp}{3\ell_p}, \quad (53)$$

which on minimization yields a cubic equation in  $\alpha_\perp$ ,

$$\alpha_\perp^{1/2} \sim (2/\pi^{1/2}) \phi_\perp g(\phi_\perp) \ell - \frac{L}{3\ell_p} \alpha_\perp^{3/2}. \quad (54)$$

The physical branch is the one for which  $\alpha_{\perp}$  is real-positive and which converges to Eq. (22) in the rigid rod limit  $\ell_p/L \rightarrow \infty$ . Compared to the case of perfectly rigid rods, a small but finite amount of backbone flexibility leads to a reduction of the orientational order of the rods for any given planar packing fraction  $\phi_{\perp}$  and rod aspect ratio  $\ell$ .

We may now simply repeat the analysis we did for the rigid rods by retaining the intralamellar orientational order parameter  $\alpha_{\perp}$  to be resolved from the cubic equation, shown previously. The total free energy of the smectic phase, again ignoring irrelevant constants, is now given by,

$$\frac{F_S}{N} \sim \ln \phi + \ln \alpha_{\perp} + \phi_{\perp} g(\phi_{\perp}) \left[ \frac{4\ell}{(\pi\alpha_{\perp})^{1/2}} + 2 \right] + \frac{L\alpha_{\perp}}{3\ell_p} - \ln [1 - \bar{\Delta}_S^{-1}(1 - \bar{\zeta} e^{-\beta W})]. \quad (55)$$

From the equation above, we identify the entropies associated with ideal gas behavior, orientational fluctuations, excluded-volume repulsion (composed of a parallel core plus an orientation-dependent part), single-rod conformational fluctuations and lamellar confinement, respectively.

### X. COMPARISON WITH EXPERIMENTAL RESULTS: COLLOIDAL VERSUS THERMOTROPIC SMECTICS

We are now in a position to recompute quantities such as the smectic layer spacing, splay and compression moduli and penetration length for stiff rods by considering a large but finite persistence  $\ell_p/L \gg 1$  and compare with experimental measurements for *fd* rods. Given that the intralamellar nematic order parameter  $\alpha_{\perp}$  is no longer strictly quadratic with rod density we must take Eq. (42) rather than Eq. (43) to compute the splay modulus. The rigid rod results shown in Fig. 3 and Fig. 5 are recovered simply by taking the limit  $\ell_p/L \rightarrow \infty$ . The limit of stability for the smectic phase at lower rod packing fraction can be gleaned from the nematic-smectic bifurcation Eq. (A12) which now also depends on the persistence length. The results (not shown here) are in line with the scenario emerging from a more elaborate theoretical analysis by van der Schoot [77], namely an increase of the nematic-smectic instability density and a simultaneous reduction of the smectic layer spacing with increasing rod flexibility. The reduction of the layer spacing with  $\ell_p$  is demonstrated in Fig. 6 where we show a comparison between our model predictions and experimental data for *fd* rods in the smectic concentration range. Recently, the penetration elastic length was measured to be  $\lambda \simeq 0.02 \pm 0.01 \mu\text{m}$  which, considering the micrometer contour length of filamentous viruses, gives  $\lambda/L \approx 0.02 \pm 0.01$  [78] which is in outstanding agreement with the predictions showcased in Fig. 5 for rigid rods. More specifically, taking an effective persistence length  $\ell_p/L = 100$  and interdigitation depth  $\bar{\zeta} = 0.5$  we find  $\lambda/L = 0.019$  in quantitative agreement with the experimental value at least for the particular concentration considered in experiment ( $\phi/\phi_{\text{NS}} = 1.36$ ) [78].

Let us now compare our findings with results reported for thermotropic smectics which are stabilized by attractive forces acting between the mesogens rather than through a trade-off between orientation versus volume-exclusion entropy. Taking

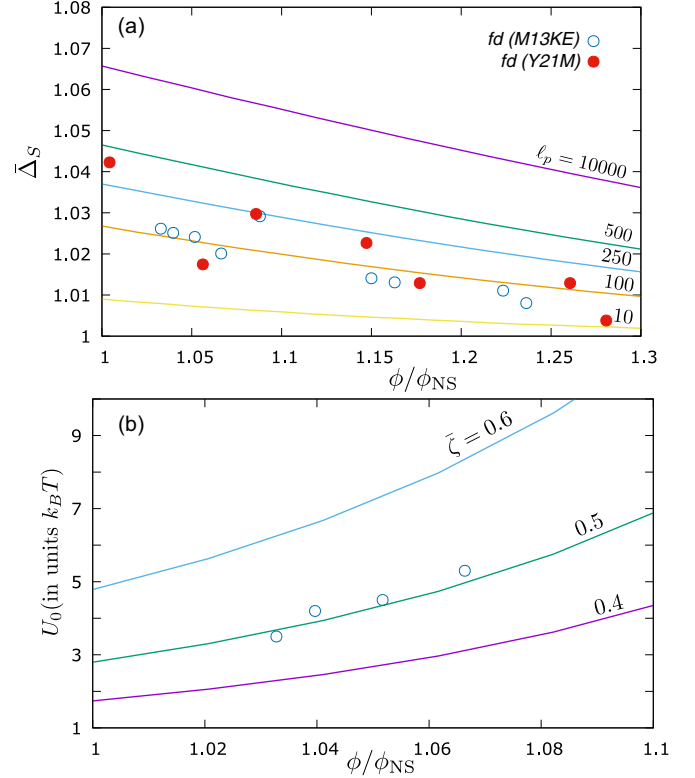


FIG. 6. Theory-experiment comparison based on data for *fd* virus rods in a smectic organization. (a) Lamellar spacing versus rod packing fraction  $\phi$  renormalized to the value at nematic-smectic coexistence  $\phi_{\text{NS}}$ . The interdigitation depth is fixed at  $\bar{\zeta} = 0.5$ . Shown are results for two different *fd* strands: M13KE ( $\ell_p/L = 3$ ) and the much stiffer Y21M ( $\ell_p/L = 10$ ). (b) Smectic potential for a number of different interdigitation depths  $\bar{\zeta} = \zeta/L$  and  $\ell_p = 250$ . Experimental data are based on M13KE.

the lamellar spacing  $\Delta_S$  as the intrinsic length scale one finds that generically  $\lambda \sim \Delta_S$ . Quoting experimental values from Refs. [48–50,79] we specify  $\lambda \sim 1$  to 7 nm with  $\Delta_S \sim 3$  nm [80]. By contrast, for colloidal smectics composed of *fd* rods,  $\lambda$  amounts to only a fraction of the lamellar spacing. The main reason behind this discrepancy is that the typical layer compressibility modulus  $B \sim 10^{3-4} \text{ N/m}^2$  for colloidal rod smectics is found to be at least three orders of magnitude smaller than the typical value  $B \sim 10^7 \text{ N/m}^2$  encountered for thermotropic smectics [48,79,81,82]. The splay constant, however, is of similar magnitude for both colloidal and thermotropic smectics. For a typical thermotropic smectic we quote from Refs. [48,79] a splay director diffusion coefficient  $K_1/\eta_s \sim 2 \times 10^{-10} \text{ m}^2/\text{s}$  which, taking a typical (splay) viscosity  $\eta_s \sim 10^{-2} \text{ Pa s}$ , leads to a modulus of about  $K_1 \sim 10 \text{ pN}$ . This value is also in agreement with the study of Bradshaw and Raynes [83]. For colloidal *fd* rods, the experimental value for the splay elastic constant is found to be about  $2 \pm 1 \text{ pN}$  [78]. This estimate is based on (1) measurement of the bend modulus  $\kappa$  of fluidlike membranes composed of a monolayer of aligned viruses [84], which gives after normalization by the lamellar spacing  $\Delta_S$ :  $K_1 = \kappa/\Delta_S \approx 1 \text{ pN}$ , and (2) the nematic splay elastic constant evaluated close to the nematic-smectic transition inferred from Odijk's scaling

prediction [Eq. (40)] for rigid hard rods [70]  $K_1 \approx 3K_2 \approx 3$  pN, where  $K_2$  is the twist elastic constant measured from unwinding the helical mesostructure of a cholesteric virus suspension under a magnetic field [85]. The experimental value is thus found to be at most an order of magnitude smaller than our prediction  $K_1 \sim 10$  pN according to Eq. (43) taking typical values for  $fd$  ( $\ell = 100$ ,  $\phi = 0.5$ ,  $D = 10$  nm, and  $\xi L^2 = 200$ ). The discrepancy could be attributed to the absence of conformational fluctuations in our treatment of the volume-exclusion entropy as well as the neglect of electrostatic interactions in our model.

## XI. CONCLUSION

Inspired by a recent upsurge in experimental work on colloidal smectics, we have proposed a microscopic theory that combines concepts from density functional and cell theory in an effort to predict the thermodynamics and elastic properties of colloidal smectic phases stabilized primarily by entropic forces due to rod volume exclusion. In our study, we focus on predicting the layer compression and bending moduli, which for colloidal smectics have scarcely been addressed thus far, and we quantify those as a function of the rod packing fraction and rod aspect ratio. The characteristic length scale associated with the ratio of the elastic moduli, called the smectic penetration length, amounts to only a fraction of the layer spacing in contrast to thermotropic smectic materials where the two length scales are found to be similar. We attribute this to the fact that smectics composed of colloidal rods experience a much smaller layer compressibility ( $B$ ) than typical thermotropic smectics whereas the energy scales associated with layer bending ( $K_1$ ) are of comparable magnitude. This illustrates that colloidal smectics have a mechanical response that is considerably different from their thermotropic counterparts with key implications for their defect topology.

We further demonstrate that introducing small degree of backbone flexibility, such as present in filamentous virus rods, leads to a reduction of the equilibrium lamellar spacing. Our predictions for the spacing, penetration length and layer “barrier-hopping” potential which governs the single-particle diffusive dynamics along the layer normal, are in quantitative agreement with experimental measurements.

Since our theory is restricted to hard-core volume exclusions alone, the effect of electrostatic repulsion and other “soft” interactions as well as the subtle role of rod flexibility in the volume-exclusion entropy is overlooked here and should be addressed in more elaborate numerical treatments including computer simulations as has been done for the semiflexible case [73,74,86]. We believe that this issue is particularly relevant for stiff but nonrigid rods with  $\ell_p > L$  such as filamentous  $fd$  virus discussed here, where backbone flexibility is usually ignored but is found to play an important role nevertheless in determining the smectic mesostructure and dynamics through the “hopping” potential [44,72]. Although  $fd$  rods are strongly charged and strictly do not interact as hard objects, their phase behavior can be mapped quite efficiently on a hard-core model using a suitable renormalization of the rod dimensions [72]. Similar recipes could be applied to other smectogenic colloidal particles provided the soft interactions are

not too strong and long-ranged. Our predictions will then be instrumental, for instance, in guiding continuum models [35–37] to classify topological defects in a wide range of lyotropic smectic materials.

## ACKNOWLEDGMENTS

We acknowledge financial support from the French National Research Agency (ANR) under Grant No. ANR-19-CE30-0024 “ViroLego.” We also kindly thank Jaydeep Mandal and Prabal Maiti from Bangalore University (India) for constructive discussions and for sharing their simulation results with us.

## APPENDIX: APPENDIX: INCIPIENT FREEZING FROM A UNIFORM NEMATIC FLUID

In this Appendix we wish to illustrate the wider applicability of the analytical rendering of the excluded volume between elongated colloidal particles proposed in Sec. III in relation to phase transitions in systems of rod and disk-shaped colloids. We use a simple stability analysis to predict the nematic-smectic or nematic-columnar transition at the level of bifurcations from a spatially uniform nematic fluid. We apply this to a number of relevant systems, namely rods and disks in 3D and rods confined to a smectic monolayer. An overview of the results is given in Table I. Details of the analysis for each specific case can be found in the paragraphs below.

The case of a monolayer rod fluid, which is relevant for thin films or strongly confined systems of elongated macromolecules, has received recent attention from density functional theory [53], experiment [87], as well as computer simulation [88]. In the latter study, for strictly flat monolayers a nematic-solid transition was identified around a packing fraction 83% independent of the aspect ratio [89]. This value is very close to our prediction (81%) listed in Table I. In the context of space-filling smectics solidification of a single smectic monolayer can be tentatively connected to the emergence of SmB order. Our results then suggests that the transition from SmA to SmB order occurs at very high packing conditions. It is likely, however, that the crossover from SmA to SmB order for strictly hard cylinders is pre-empted by transitions to solid phases that are thermodynamically more stable under these conditions [12,17,18].

For slender rods in a 3D bulk nematic, the results are in good agreement with computer simulation results where the nematic-smectic transition is found to vary only weakly with aspect ratio [17,18]. This complies with the “rule-of-thumb” that a critical packing fraction of a little over 40% seems required to stabilize a frozen state in hard-body systems, irrespective of their shape [15,90]. For strictly parallel rods the transition would happen at a far too low packing fraction, namely  $\phi^* = 0.34$ . We conclude that orientational fluctuations play an essential role in steering the transition towards a realistic density range.

Our treatment of the excluded-volume correlations can be further tested by scrutinizing the nematic-columnar transition for thin disks ( $L/D \ll 1$ ). For strictly parallel particles the excluded volume is *identical* to the one for elongated cylinders so that a second-virial theory would not be able to distinguish

TABLE I. Nematic-solid (NX), nematic-smectic (NS), and nematic-columnar (NC) freezing of hard cylinders. Overview of bulk freezing transitions in terms of the bifurcation packing fraction  $\phi^*$  for hard cylinders in a two-dimensional monolayer fluid and in three dimension bulk nematics. The corresponding wave number defining the typical distance between adjacent smectic layers or columns is indicated by  $q^*$ . The relevant transition values are indicated in bold.

Transition	$\phi^*$ parallel	$\phi^*$ freely rotating	$q^*$ parallel	$q^*$ freely rotating
NX monolayer rods	<b>0.58</b>	<b>0.81</b>	<b>5.13/D</b>	<b>5.13/D</b>
NS rods in 3D	<b>0.34</b>	<b>0.40</b>	<b>4.49/L</b>	<b>4.86/L</b>
NC rods in 3D	0.44	0.73	5.13/D	5.13/D
NS disks in 3D	<b>0.34</b>	0.75	<b>4.49/L</b>	4.49/L
NC disks in 3D	0.44	<b>0.61</b>	5.13/D	<b>5.45/D</b>

between oblate and prolate cylinders. For disks, however, we know from simulations [15,16,91] and experiments on clay platelets [92–94] that the nematic-columnar transition preempts the nematic-smectic transition whereas second-virial theory for parallel cylinders predicts that columnar order is *always* metastable with respect to the smectic phase [95]. While it is known since Onsager’s seminal work [13] that second-virial approaches generally fall short in quantitatively describing discotic systems [96], we argue that the orientation fluctuations of the disks (ignored in parallel-core models [12]) also play a key role in favoring columnar over smectic ordering. This is corroborated by our theory (see Table I) in that freely rotating hard disks favor columnar over smectic order, even though the critical packing fraction at the nematic-columnar transition ( $\phi^* = 0.61$ ) is overestimated by our theory in line with earlier theoretical findings [97].

### 1. Freezing of a monolayer rod fluid

When the intralamellar density exceeds a critical value the monolayer fluid is expected to transition into a solid characterized by in-plane periodic order following some Bravais lattice that we may parametrize by a (combination of) wave vectors  $\mathbf{q}_\perp$ . Close to the nematic-solid (NX) transition, that we assume to be of a second-order nature [88,89], the one-body density can be written in terms of the reference solution for the fluid state and a periodic density modulation with infinitesimally small amplitude  $\epsilon \ll 1$  [10,95,98],

$$\rho(\mathbf{r}_\perp; \omega) = \rho_\perp [f(\omega) + \epsilon f_q(\omega) e^{i\mathbf{q}_\perp \cdot \mathbf{r}_\perp}], \quad (\text{A1})$$

where the orientation distribution  $f_q(\omega) \neq f(\omega)$  in general depends on the wave vector  $\mathbf{q}_\perp$  of the in-plane density modulation.

Next, we linearize the grand potential Eq. (2) for arbitrarily small amplitude  $\epsilon$ . The result is a bifurcation condition that identifies the point where spatially nonuniform distributions for the planar one-body density branch off from the fluid solution,

$$f_q(\omega) = \rho_\perp f(\omega) \int d\omega' f_q(\omega') \hat{\mathcal{K}}(\mathbf{q}_\perp). \quad (\text{A2})$$

The key quantity is the kernel  $\hat{\mathcal{K}}$  that combines the hard-core volume-exclusion contributions discussed in the main text,

$$\rho_\perp \hat{\mathcal{K}}(\mathbf{q}_\perp) = -8\phi_\perp g(\phi_\perp) \left\{ \frac{J_1(q_\perp)}{q_\perp} + \mathcal{F}(\mathbf{q}_\perp) \right\}. \quad (\text{A3})$$

The first terms denotes the parallel hard-core term while the second term accounts for the orientational fluctuations of the rods and features an explicit coupling between the incipient density modulation and the azimuthal rod angle,

$$\mathcal{F}(\mathbf{q}_\perp) = \frac{\gamma \ell}{3\pi} \sum_{n=1}^3 j_0 \left[ \frac{q_\perp}{2} \ell (\theta \mathbf{a}_n \cdot \boldsymbol{\omega}_\perp - \theta' \mathbf{a}_n \cdot \boldsymbol{\omega}'_\perp) \right], \quad (\text{A4})$$

with  $\boldsymbol{\omega}_\perp = (\sin \varphi, \cos \varphi, 0)$ . Here the density modulation describes, for instance, a hexagonal Bravais lattice with primitive vectors  $\mathbf{a}_1 = (\sqrt{3}, 1)/2$ ,  $\mathbf{a}_2 = (-\sqrt{3}, 1)/2$ , and  $\mathbf{a}_3 = (0, 1)$ . Other crystal symmetries may be probed likewise [99].

Symmetry-breaking solutions deviating from a uniform fluid towards a solid state may be probed from the condition Eq. (A2). In the simplest case, we assume that the orientational distribution does *not respond* to the incipient density modulation and obeys a Gaussian form Eq. (19). This amounts to replacing in Eq. (A2),

$$f_q(\omega) = f_G(\omega). \quad (\text{A5})$$

The bifurcation condition Eq. (A2) is then equivalent to a divergence of the static structure factor indicating a loss of local stability of the monolayer fluid,

$$S^{-1}(q_\perp) = 1 + 8\phi_\perp g(\phi_\perp) \left\{ \frac{J_1(q_\perp)}{q_\perp} + \langle \langle \mathcal{F}(\mathbf{q}_\perp; \cdot) \rangle \rangle \right\} = 0. \quad (\text{A6})$$

The brackets denote a double Gaussian average defined in the main text. The bifurcation solution of Eq. (A6) then corresponds to the lowest (real-positive) value of  $\phi_\perp^*$  with the associated wave number indicated by  $q_\perp^*$ . The averages of the interrod angles are known analytically in the asymptotic limit and are given in Eq. (21). This is not the case, however, for the angular average of  $\mathcal{F}$  where the polar and azimuthal angles are strongly convoluted with the wave vector  $\mathbf{q}_\perp$ . To make headway we assume that the polar angles of the rods are “frozen” at a small value  $\theta = \theta' = \theta_c \ll 1$  while fluctuations in the azimuthal angles remain *a priori* unrestricted. Next we substitute the asymptotic expression  $\gamma \approx (\theta^2 + \theta'^2 - 2\theta\theta' \cos \Delta\varphi)^{1/2} \sim 2^{1/2} \theta_c \sqrt{1 - \cos \Delta\varphi}$  with  $\Delta\varphi = \varphi - \varphi'$ . Technically this amounts to replacing the Gaussian orientational probability by an even simpler factorized form,

$$f_G(\omega) \sim \frac{\delta(\theta - \theta_c)}{\sin \theta_c} \frac{1}{2\pi}. \quad (\text{A7})$$

Since the azimuthal fluctuations are presumed unaffected by the density modulation, the three lattice vector contributions

$\mathbf{a}_n$  are equal. Using the result  $\frac{2^{1/2}}{2\pi} \int_0^{2\pi} dx \sqrt{1 - \cos x} = 4/\pi$ , the problem reduces to a single azimuthal average,

$$\langle\langle \mathcal{F}(\mathbf{q}_\perp) \rangle\rangle \sim \frac{4}{\pi^2} (\ell\theta_c) \int_0^{2\pi} \frac{d\varphi}{2\pi} j_0 \left[ \frac{q_\perp}{2} (\ell\theta_c) \cos \varphi \right]. \quad (\text{A8})$$

We may link the constrained polar angle  $\theta_c$  to the nematic order parameter  $\alpha_\perp$  and rod packing fraction  $\phi_\perp$  via,

$$\ell\theta_c \sim \ell \langle \theta^2 \rangle_{fg}^{1/2} \sim (2\ell^2/\alpha_\perp)^{1/2}. \quad (\text{A9})$$

We invoke the quadratic relationship with the packing fraction  $\phi_\perp$  Eq. (22) and find,

$$\ell\theta_c \sim \left(\frac{\pi}{2}\right)^{1/2} \frac{1}{\phi_\perp g(\phi_\perp)}, \quad (\text{A10})$$

independent from the rod aspect ratio  $\ell$ . A trivial reference case is a system of perfectly parallel hard cylinders previously analyzed by Mulder [95]. We set  $\theta_c = 0$  and  $f(\omega) = \delta(\omega)$  and find that the structure factor Eq. (A6) has a pole at  $\phi_\perp \approx 0.58$  and  $q_\perp \approx 5.13$ . The presence of orientational fluctuations expressed by Eq. (A8)] leads to a much higher transition values namely  $\phi_\perp \approx 0.81$  while leaving the critical wave number unchanged ( $q_\perp \approx 0.513$ ). The results have been tabulated in Table I.

## 2. Smectic versus columnar freezing of hard rods

In order to further test our theory, we consider the much more widely studied system of rigid hard cylinders in 3D [10,12,14,17,18]. When exceeding a certain critical packing fraction these systems are known to form a smectic-A phase emerging from a nematic fluid. In our approach, the hard-body interaction between the cylinders can be approximated by a parallel hard-core contribution supplemented with a fluctuation term that depends on the rod orientations. Ignoring correlations between end-caps which should be negligible for sufficiently long rods  $\ell = L/D \gg 1$ , we find that FT of the excluded volume reads as follows,

$$\begin{aligned} \hat{\mathcal{K}}(\mathbf{q}) &\approx -2\pi LD^2 j_0(q_\parallel L) \frac{J_1(q_\perp D)}{\frac{1}{2}q_\perp D} \\ &- 2L^2 D |\sin \gamma| j_0 \left( \frac{L}{2} \mathbf{q} \cdot \boldsymbol{\omega} \right) j_0 \left( \frac{L}{2} \mathbf{q} \cdot \boldsymbol{\omega}' \right) + \mathcal{O}(D^3). \end{aligned} \quad (\text{A11})$$

Assuming the principal director to point along the  $z$  axis of the laboratory frame we write  $q_\parallel = \mathbf{q} \cdot \hat{\mathbf{z}}$  and  $q_\perp = \mathbf{q} \cdot \hat{\mathbf{x}} = \mathbf{q} \cdot \hat{\mathbf{y}}$ . Similarly to the monolayer case we may probe bifurcations from the uniform nematic fluid towards, for instance, a smectic structure for which  $\mathbf{q} \cdot \boldsymbol{\omega} = q_\parallel \cos \theta$  and  $q_\perp = 0$ . Then, the nematic-smectic (NS) bifurcation in the asymptotic limit of strong alignment follows from,

$$S_{\text{NS}}^{-1}(q_\parallel) \sim 1 + 8\phi g(\phi) \left[ j_0(q_\parallel L) + \frac{1}{\pi} \ell \langle \langle \gamma \rangle \rangle j_0^2 \left( \frac{q_\parallel L}{2} \right) \right] = 0. \quad (\text{A12})$$

Using the Gaussian approximation we write for the double averaged angle,

$$\ell \langle \langle \gamma \rangle \rangle \sim \frac{\pi}{2g(\phi)\phi}. \quad (\text{A13})$$

The solution is  $\phi^* = 0.403$  and  $q_\parallel^* L = 4.86$  independent of the rod aspect ratio  $\ell$ .

To finalize our analysis we also explore the possibility of a nematic-columnar transition for rods in which case a density modulation develops across the plane transverse to the nematic director  $\mathbf{q} = (q_\perp, 0, 0)$ . In the asymptotic limit of near-parallel rods we find  $D\mathbf{q} \cdot \boldsymbol{\omega} \sim \mathcal{O}(q_\perp D\theta) \sim 0$  so that the divergence criterion for the structure factor reads,

$$S_{\text{NC}}^{-1}(q_\perp) \sim 1 + 8\phi g(\phi) \left[ \frac{J_1(q_\perp D)}{\frac{1}{2}q_\perp D} + \frac{1}{\pi} \ell \langle \langle \gamma \rangle \rangle \right] = 0, \quad (\text{A14})$$

with solution  $\phi^* = 0.73$  and  $q_\perp^* D = 5.14$ . This demonstrates that the nematic-smectic transition strongly pre-empt the columnar phase as is well known from computer simulation [14,17,18] and experiment [25,43].

## 3. Smectic versus columnar freezing of hard disks

We finish our analysis by addressing freezing instabilities in fluids of thin cylindrical disks with a large diameter-to-thickness ratio  $D/L \gg 1$ . The orientational fluctuation contribution to the excluded volume for thin disks is much more complicated than the one for rods and has been computed by one of us [100],

$$\begin{aligned} \hat{\mathcal{K}}(\boldsymbol{\omega}, \boldsymbol{\omega}') &\approx -2\pi LD^2 j_0(q_\parallel L) \frac{J_1(q_\perp D)}{\frac{1}{2}q_\perp D} \\ &- \frac{\pi}{4} D^3 |\sin \gamma| \left[ A_1 \frac{J_1(\bar{q}_2)}{\frac{1}{2}\bar{q}_2} + A_2 \frac{J_1(\bar{q}_1)}{\frac{1}{2}\bar{q}_1} \right] \\ &+ \mathcal{O}(DL^2), \end{aligned} \quad (\text{A15})$$

with  $\bar{q}_n = \sqrt{(\frac{D}{2}\mathbf{q} \cdot \hat{\mathbf{v}})^2 + (\frac{D}{2}\mathbf{q} \cdot \hat{\mathbf{w}}_n)^2}$  and,

$$\begin{aligned} A_n &= \frac{1}{2} \int_{-1}^1 dt \cos \left( \frac{D}{2} t \mathbf{q} \cdot \hat{\mathbf{w}}_1 \right) \cos \left( \frac{D}{2} \sqrt{1-t^2} \mathbf{q} \cdot \hat{\mathbf{v}} \right) \\ &\approx J_0(\bar{q}_n), \end{aligned} \quad (\text{A16})$$

with  $\hat{\mathbf{v}} = (\boldsymbol{\omega} \times \boldsymbol{\omega}')/|\sin \gamma|$  and  $\hat{\mathbf{w}}_n = \boldsymbol{\omega}_n \times \hat{\mathbf{v}}$  two auxiliary unit vectors associated with the particle frame of each disk. It is easily verified that the zero-wave-number limit ( $\bar{q}_n = 0$ ) of the second contribution above yields  $-\frac{\pi}{2} D^3 |\sin \gamma|$  which corresponds to (minus) the excluded volume between two infinitely thin hard disks of diameter  $D$ . Taking the asymptotic limit of small polar angles and considering only density modulations in the  $xy$  plane perpendicular to the nematic director ( $q_\parallel = 0$ ) we find that the orientation-dependent arguments of the Bessel functions can be expressed as,

$$\bar{q} \sim \pm q_\perp D \left( \frac{\theta' - \theta \cos \Delta\varphi}{2\gamma} \right). \quad (\text{A17})$$

The sign is irrelevant here given that both Bessel functions above are even functions. The next step is to preaverage the term between brackets over the disk orientations which in the Gaussian approximations gives a mere constant of  $\mathcal{O}(1)$ , namely  $\langle \langle (\theta' - \theta \cos \Delta\varphi)/2\gamma \rangle \rangle = c_0 \approx 0.3$ . Taking all this into account we find that the divergence of the structure factor at the nematic-columnar (NC) transition can be established

from the following simple condition,

$$S_{NC}^{-1}(q_{\perp}) \sim 1 + 8\phi g(\phi) \left[ \frac{J_1(q_{\perp}D)}{\frac{1}{2}q_{\perp}D} + \frac{1}{2}\delta\langle\langle\gamma\rangle\rangle \frac{J_0(c_0q_{\perp}D)J_1(c_0q_{\perp}D)}{c_0q_{\perp}D} \right] = 0, \quad (\text{A18})$$

where  $\delta = D/L \gg 1$  defines the aspect-ratio of the disk. Applying the Gaussian scaling arguments invoked for rods to the case of disks we find,

$$\delta\langle\langle\gamma\rangle\rangle \sim \frac{2}{g(\phi)\phi}, \quad (\text{A19})$$

which renders the results independent of the disk aspect ratio. The bifurcation criterion is easily resolved numerically and yields  $\phi^* = 0.61$  and  $q_{\parallel}^*L = 5.45$ . Similarly, we may probe the nematic-smectic transition from taking  $\mathbf{q} = q_{\parallel}\hat{\mathbf{z}}$ . Then, in the asymptotic limit we infer that  $\bar{q} \sim \mathcal{O}(q_{\parallel}L\theta)$  is small and can be set to zero in good approximation. The condition for the nematic-smectic transition for disks then reads,

$$S_{NS}^{-1}(q_{\parallel}) \sim 1 + 8\phi g(\phi) \left[ j_0(q_{\parallel}L) + \frac{1}{2}\delta\langle\langle\gamma\rangle\rangle \right] = 0, \quad (\text{A20})$$

which has a solution  $\phi^* = 0.75$  and  $q_{\parallel}^*L = 4.49$ . The results are summarized in Table I.

- 
- [1] P.-G. De Gennes and J. Prost, *The Physics of Liquid Crystals* (Oxford University Press, Oxford, 1993), Vol. 83.
- [2] W. H. De Jeu, *Physical Properties of Liquid Crystalline Materials* (CRC Press, Boca Raton, FL, 1980), Vol. 1.
- [3] A. Doostmohammadi and B. Ladoux, Physics of liquid crystals in cell biology, *Trends Cell Biol.* **32**, 140 (2022).
- [4] S. A. Jewell, Living systems and liquid crystals, *Liq. Cryst.* **38**, 1699 (2011).
- [5] M. Mitov, Cholesteric liquid crystals in living matter, *Soft Matter* **13**, 4176 (2017).
- [6] W. Helfrich, Out-of-plane fluctuations of lipid bilayers, *Z. Naturforsch. C* **30**, 841 (1975).
- [7] W. Helfrich, Steric interaction of fluid membranes in multilayer systems, *Z. Naturforsch. A* **33**, 305 (1978).
- [8] W. H. de Jeu, B. I. Ostrovskii, and A. N. Shalaginov, Structure and fluctuations of smectic membranes, *Rev. Mod. Phys.* **75**, 181 (2003).
- [9] G. J. Vroege and H. N. W. Lekkerkerker, Phase transitions in lyotropic colloidal and polymer liquid crystals, *Rep. Prog. Phys.* **55**, 1241 (1992).
- [10] M. P. Allen, G. T. Evans, D. Frenkel, and B. M. Mulder, Hard convex body fluids, *Adv. Chem. Phys.* **86**, 1 (1993).
- [11] S. Singh, Phase transitions in liquid crystals, *Phys. Rep.* **324**, 107 (2000).
- [12] L. Mederos, E. Velasco, and Y. Martinez-Raton, Hard-body models of bulk liquid crystals, *J. Phys.: Condens. Matter* **26**, 463101 (2014).
- [13] L. Onsager, The effects of shape on the interaction of colloidal particles, *Ann. N. Y. Acad. Sci.* **51**, 627 (1949).
- [14] D. Frenkel, H. N. W. Lekkerkerker, and A. Stroobants, Thermodynamic stability of a smectic phase in a system of hard rods, *Nature (London)* **332**, 822 (1988).
- [15] D. Frenkel, Invited lecture: Columnar ordering as an excluded-volume effect, *Liq. Cryst.* **5**, 929 (1989).
- [16] J. A. C. Veerman and D. Frenkel, Phase behavior of disklike hard-core mesogens, *Phys. Rev. A* **45**, 5632 (1992).
- [17] S. C. McGrother, D. C. Williamson, and G. Jackson, A re-examination of the phase diagram of hard spherocylinders, *J. Chem. Phys.* **104**, 6755 (1996).
- [18] P. Bolhuis and D. Frenkel, Tracing the phase boundaries of hard spherocylinders, *J. Chem. Phys.* **106**, 666 (1997).
- [19] D. A. King and R. D. Kamien, What promotes smectic order: Applying mean field theory to the ends, [arXiv:2301.00267](https://arxiv.org/abs/2301.00267) [cond-mat.soft].
- [20] R. van Roij, P. Bolhuis, B. Mulder, and D. Frenkel, Transverse interlayer order in lyotropic smectic liquid crystals, *Phys. Rev. E* **52**, R1277 (1995).
- [21] E. Grelet, M. P. Lettinga, M. Bier, R. Van Roij, and P. van der Schoot, Dynamical and structural insights into the smectic phase of rod-like particles, *J. Phys.: Condens. Matter* **20**, 494213 (2008).
- [22] A. Patti, D. El Masri, R. van Roij, and M. Dijkstra, Collective diffusion of colloidal hard rods in smectic liquid crystals: Effect of particle anisotropy, *J. Chem. Phys.* **132**, 224907 (2010).
- [23] M. Chiappini, E. Grelet, and M. Dijkstra, Speeding up Dynamics by Tuning the Noncommensurate Size of Rodlike Particles in a Smectic Phase, *Phys. Rev. Lett.* **124**, 087801 (2020).
- [24] X. Wen, R. B. Meyer, and D. L. D. Caspar, Observation of Smectic-a Ordering in a Solution of Rigid-Rod-Like Particles, *Phys. Rev. Lett.* **63**, 2760 (1989).
- [25] R. B. Meyer, Ordered phases in colloidal suspensions of tobacco mosaic virus, in *Dynamics and Patterns in Complex Fluids* (Springer, Berlin, 1990), pp. 62–73.
- [26] S. N. Hosseini, A. Grau-Carbonell, A. G. Nikolaenkova, X. Xie, X. Chen, A. Imhof, A. van Blaaderen, and P. J. Baesjou, Smectic liquid crystalline titanium dioxide nanorods: Reducing attractions by optimizing ligand density, *Adv. Funct. Mater.* **30**, 2005491 (2020).
- [27] H. Maeda and Y. Maeda, Liquid Crystal Formation in Suspensions of Hard Rodlike Colloidal Particles: Direct Observation of Particle Arrangement and Self-Ordering Behavior, *Phys. Rev. Lett.* **90**, 018303 (2003).
- [28] G. J. Vroege, D. M. E. Thies-Weesie, A. V. Petukhov, B. J. Lemaire, and P. Davidson, Smectic liquid-crystalline order in suspensions of highly polydisperse goethite nanorods, *Adv. Mater.* **18**, 2565 (2006).
- [29] C. Querner, M. D. Fischbein, P. A. Heiney, and M. Drndić, Millimeter-scale assembly of cds nanorods into smectic superstructures by solvent drying kinetics, *Adv. Mater.* **20**, 2308 (2008).
- [30] C. Hamon, M. Postic, E. Mazari, T. Bizien, C. Dupuis, P. Even-Hernandez, A. Jimenez, L. Courbin, C. Gosse, F. Artzner, and V. Marchi-Artzner, Three-dimensional self-assembling of gold nanorods with controlled macroscopic shape and local smectic b order, *ACS Nano* **6**, 4137 (2012).
- [31] A. Kuijk, D. V. Byelov, A. V. Petukhov, A. Van Blaaderen, and A. Imhof, Phase behavior of colloidal silica rods, *Faraday Discuss.* **159**, 181 (2012).

- [32] P. A. Monderkamp, R. Wittmann, L. B. G. Cortes, D. G. A. L. Aarts, F. Smallenburg, and H. Löwen, Topology of Orientational Defects in Confined Smectic Liquid Crystals, *Phys. Rev. Lett.* **127**, 198001 (2021).
- [33] R. Wittmann, L. B. G. Cortes, H. Löwen, and D. G. A. L. Aarts, Particle-resolved topological defects of smectic colloidal liquid crystals in extreme confinement, *Nat. Commun.* **12**, 623 (2021).
- [34] R. Wittmann, P. A. Monderkamp, J. Xia, L. B. G. Cortes, I. Grobas, P. E. Farrell, D. G. A. L. Aarts, and H. Löwen, Smectic structures in button-like confinements: Experiment and theory, [arXiv:2303.01425](https://arxiv.org/abs/2303.01425).
- [35] J. Xia, S. MacLachlan, T. J. Atherton, and P. E. Farrell, Structural Landscapes in Geometrically Frustrated Smectics, *Phys. Rev. Lett.* **126**, 177801 (2021).
- [36] J. Paget, U. Alberti, M. G. Mazza, A. J. Archer, and T. N. Shendruk, Smectic layering: Landau theory for a complex-tensor order parameter, *J. Phys. A: Math. Theor.* **55**, 354001 (2022).
- [37] J. Paget, M. G. Mazza, A. J. Archer, and T. N. Shendruk, Complex-tensor theory of simple smectics, *Nat. Commun.* **14**, 1048 (2023).
- [38] R. Hentschke, M. P. Taylor, and J. Herzfeld, Equation of state for parallel hard spherocylinders, *Phys. Rev. A* **40**, 1678 (1989).
- [39] H. Graf, H. Löwen, and M. Schmidt, Cell theory for the phase diagram of hard spherocylinders, in *Optical Methods and Physics of Colloidal Dispersions* (Springer, Berlin, 1997), pp. 177–179.
- [40] H. Graf and H. Löwen, Phase diagram of tobacco mosaic virus solutions, *Phys. Rev. E* **59**, 1932 (1999).
- [41] H. H. Wensink, Equation of State of a Dense Columnar Liquid Crystal, *Phys. Rev. Lett.* **93**, 157801 (2004).
- [42] V. F. D. Peters, M. Vis, H. H. Wensink, and R. Tuinier, Algebraic equations of state for the liquid crystalline phase behavior of hard rods, *Phys. Rev. E* **101**, 062707 (2020).
- [43] Z. Dogic and S. Fraden, Smectic Phase in a Colloidal Suspension of Semiflexible Virus Particles, *Phys. Rev. Lett.* **78**, 2417 (1997).
- [44] M. P. Lettinga and E. Grelet, Self-Diffusion of Rodlike Viruses Through Smectic Layers, *Phys. Rev. Lett.* **99**, 197802 (2007).
- [45] E. Pouget, E. Grelet, and M. P. Lettinga, Dynamics in the smectic phase of stiff viral rods, *Phys. Rev. E* **84**, 041704 (2011).
- [46] A. Repula, M. Oshima Menegon, C. Wu, P. van der Schoot, and E. Grelet, Directing Liquid Crystalline Self-Organization of Rodlike Particles through Tunable Attractive Single Tips, *Phys. Rev. Lett.* **122**, 128008 (2019).
- [47] C. Ollinger, D. Constantin, J. Seeger, and T. Salditt, Lipid membranes on a surface grating studied by neutron reflectometry, *Europhys. Lett.* **71**, 311 (2005).
- [48] H. Birecki, R. Schaetzing, F. Rondelez, and J. D. Litster, Light-Scattering Study of a Smectic-A Phase Near the Smectic-A- Nematic Transition, *Phys. Rev. Lett.* **36**, 1376 (1976).
- [49] H.-J. Fromm, High resolution study of the compression modulus B in the vicinity of the nematic-smectic A transition in 60CB/80CB mixtures, *J. Phys. France* **48**, 647 (1987).
- [50] M. E. Lewis, I. Khan, H. Vithana, A. Baldwin, D. L. Johnson, and M. E. Neubert, Light scattering near the nematic–smectic-a liquid-crystal phase transition, *Phys. Rev. A* **38**, 3702 (1988).
- [51] A. Poniewierski and R. Holyst, Nematic alignment at a solid substrate: The model of hard spherocylinders near a hard wall, *Phys. Rev. A* **38**, 3721 (1988).
- [52] R. van Roij, Simple theories of complex fluids, Ph.D. thesis, Utrecht University, 1996.
- [53] M. Oettel, M. Klopotek, M. Dixit, E. Empting, T. Schilling, and H. Hansen-Goos, Monolayers of hard rods on planar substrates. I. equilibrium, *J. Chem. Phys.* **145**, 074902 (2016).
- [54] J. D. Parsons, Nematic ordering in a system of rods, *Phys. Rev. A* **19**, 1225 (1979).
- [55] S.-D. Lee, A numerical investigation of nematic ordering based on a simple hard-rod model, *J. Chem. Phys.* **87**, 4972 (1987).
- [56] J. Herzfeld, A. E. Berger, and J. W. Wingate, A highly convergent algorithm for computing the orientation distribution functions of rodlike particles, *Macromolecules* **17**, 1718 (1984).
- [57] R. van Roij, The isotropic and nematic liquid crystal phase of colloidal rods, *Eur. J. Phys.* **26**, S57 (2005).
- [58] T. Odijk, Theory of lyotropic polymer liquid crystals, *Macromolecules* **19**, 2313 (1986).
- [59] L. Alvarez, M. P. Lettinga, and E. Grelet, Fast Diffusion of Long Guest Rods in a Lamellar Phase of Short Host Particles, *Phys. Rev. Lett.* **118**, 178002 (2017).
- [60] H. Reiss, H. L. Frisch, and J. L. Lebowitz, Statistical mechanics of rigid spheres, *J. Chem. Phys.* **31**, 369 (1959).
- [61] J.-P. Hansen and I. R. McDonald, Theory of simple liquids, *Phys. Today* **41**, 89 (1988).
- [62] E. Helfand, H. L. Frisch, and J. L. Lebowitz, Theory of the two- and one-dimensional rigid sphere fluids, *J. Chem. Phys.* **34**, 1037 (1961).
- [63] M. Baus and J.-L. Colot, Thermodynamics and structure of a fluid of hard rods, disks, spheres, or hyperspheres from rescaled virial expansions, *Phys. Rev. A* **36**, 3912 (1987).
- [64] J. Han and J. Herzfeld, An avoidance model for short-range order induced by soft repulsions in systems of rigid rods, *MRS Online Proc. Lib.* **463**, (1996).
- [65] E. M. Kramer and J. Herzfeld, Avoidance model for soft particles. i. charged spheres and rods beyond the dilute limit, *J. Chem. Phys.* **110**, 8825 (1999).
- [66] J. A. Barker and D. Henderson, What is “liquid”? Understanding the states of matter, *Rev. Mod. Phys.* **48**, 587 (1976).
- [67] T. Odijk, Osmotic pressure of a nematic solution of polydisperse rod-like macromolecules, *Liq. Cryst.* **1**, 97 (1986).
- [68] C. Ligoure, G. Bouglet, G. Porte, and O. Diat, Smectic compressibility of polymer-containing lyotropic lamellar phases: An experimental tool to study the thermodynamics of polymer confinement, *J. Phys. II* **7**, 473 (1997).
- [69] J. P. Straley, Theory of piezoelectricity in nematic liquid crystals, and of the cholesteric ordering, *Phys. Rev. A* **14**, 1835 (1976).
- [70] T. Odijk, Elastic constants of nematic solutions of rod-like and semi-flexible polymers, *Liq. Cryst.* **1**, 553 (1986).
- [71] E. Barry, D. Beller, and Z. Dogic, A model liquid crystalline system based on rodlike viruses with variable chirality and persistence length, *Soft Matter* **5**, 2563 (2009).

- [72] E. Grelet, Hard-Rod Behavior in Dense Mesophases of Semi-flexible and Rigid Charged Viruses, *Phys. Rev. X* **4**, 021053 (2014).
- [73] A. Milchev, S. A. Egorov, K. Binder, and A. Nikoubashman, Nematic order in solutions of semiflexible polymers: Hairpins, elastic constants, and the nematic-smectic transition, *J. Chem. Phys.* **149**, 174909 (2018).
- [74] A. Milchev, A. Nikoubashman, and K. Binder, The smectic phase in semiflexible polymer materials: A large scale molecular dynamics study, *Comput. Mater. Sci.* **166**, 230 (2019).
- [75] A. R. Khokhlov and A. N. Semenov, Liquid-crystalline ordering in the solution of partially flexible macromolecules, *Physica A* **112**, 605 (1982).
- [76] T. Kuriabova, M. D. Bettegton, and M. A. Glaser, Linear aggregation and liquid-crystalline order: Comparison of monte carlo simulation and analytic theory, *J. Mater. Chem.* **20**, 10366 (2010).
- [77] P. van der Schoot, The nematic-smectic transition in suspensions of slightly flexible hard rods, *J. Phys. II France* **6**, 1557 (1996).
- [78] A. Repula and E. Grelet, Elementary Edge and Screw Dislocations Visualized at the Lattice Periodicity Level in the Smectic Phase of Colloidal Rods, *Phys. Rev. Lett.* **121**, 097801 (2018).
- [79] R. Ribotta, D. Salin, and G. Durand, Quasielastic Rayleigh Scattering in a Smectic-A Crystal, *Phys. Rev. Lett.* **32**, 6 (1974).
- [80] D. Davidov, C. R. Safinya, M. Kaplan, S. S. Dana, R. Schaetzing, R. J. Birgeneau, and J. D. Litster, High-resolution x-ray and light-scattering study of critical behavior associated with the nematic—smectic-A transition in 4-cyano-4'-octylbiphenyl, *Phys. Rev. B* **19**, 1657 (1979).
- [81] M. Benzekri, T. Claverie, J. P. Marcerou, and J. C. Rouillon, Nonvanishing of the Layer Compressional Elastic Constant at the Smectic-A-To-Nematic Phase Transition: A Consequence of Landau-Peierls Instability? *Phys. Rev. Lett.* **68**, 2480 (1992).
- [82] G. Carbone, B. Zappone, R. Barberi, R. Bartolino, and I. Musevic, Direct nanomechanical measurement of layer thickness and compressibility of smectic liquid crystals, *Phys. Rev. E* **83**, 051707 (2011).
- [83] M. J. Bradshaw and E. P. Raynes, The bend and splay elastic constants on approaching an injected smectic phase, *Mol. Cryst. Liq. Cryst.* **99**, 107 (1983).
- [84] E. Barry and Z. Dogic, Entropy driven self-assembly of non-amphiphilic colloidal membranes, *Proc. Natl. Acad. Sci. USA* **107**, 10348 (2010).
- [85] Zvonimir Dogic and Seth Fraden, Cholesteric phase in virus suspensions, *Langmuir* **16**, 7820 (2000).
- [86] B. De Braaf, M. Oshima Menegon, S. Paquay, and P. van der Schoot, Self-organisation of semi-flexible rod-like particles, *J. Chem. Phys.* **147**, 244901 (2017).
- [87] M. Klopotek, H. Hansen-Goos, M. Dixit, T. Schilling, F. Schreiber, and M. Oettel, Monolayers of hard rods on planar substrates. ii. growth, *J. Chem. Phys.* **146**, 084903 (2017).
- [88] D. Rajendra, J. Mandal, Y. Hatwalne, and P. K. Maiti, Packing and emergence of the ordering of rods in a spherical monolayer, *Soft Matter* **19**, 137 (2022).
- [89] J. Mandal and P. K. Maiti (private communication, 2022).
- [90] D. Frenkel, Order through entropy, *Nat. Mater.* **14**, 9 (2015).
- [91] M. Marechal, A. Cuetos, B. Martínez-Haya, and M. Dijkstra, Phase behavior of hard colloidal platelets using free energy calculations, *J. Chem. Phys.* **134**, 094501 (2011).
- [92] F. M. van der Kooij, K. Kassapidou, and H. N. W. Lekkerkerker, Liquid crystal phase transitions in suspensions of polydisperse plate-like particles, *Nature (London)* **406**, 868 (2000).
- [93] M. C. D. Mourad, A. V. Petukhov, G. J. Vroege, and H. N. W. Lekkerkerker, Lyotropic hexagonal columnar liquid crystals of large colloidal gibbsite platelets, *Langmuir* **26**, 14182 (2010).
- [94] P. Davidson and J.-C. P. Gabriel, Mineral liquid crystals, *Curr. Opin. Colloid Interf. Sci.* **9**, 377 (2005).
- [95] B. Mulder, Density-functional approach to smectic order in an aligned hard-rod fluid, *Phys. Rev. A* **35**, 3095 (1987).
- [96] X.-M. You, A. Yu Vlasov, and A. J. Masters, The equation of state of isotropic fluids of hard convex bodies from a high-level virial expansion, *J. Chem. Phys.* **123**, 034510 (2005).
- [97] H. H. Wensink and H. N. W. Lekkerkerker, Phase diagram of hard colloidal platelets: A theoretical account, *Mol. Phys.* **107**, 2111 (2009).
- [98] H. Xu, H. N. W. Lekkerkerker, and M. Baus, Nematic-smectic a and nematic-solid transitions of parallel hard spherocylinders from density functional theory, *Europhys. Lett.* **17**, 163 (1992).
- [99] M. Baus, Statistical mechanical theories of freezing: An overview, *J. Stat. Phys.* **48**, 1129 (1987).
- [100] H. H. Wensink and E. Trizac, Generalized onsager theory for strongly anisometric patchy colloids, *J. Chem. Phys.* **140**, 024901 (2014).